Additive Manufacturing for Tissue Engineering

Solaleh Miar, Ashkan Shafiee, Teja Guda, and Roger Narayan

Contents

S. Miar · T. Guda
Department of Biomedical Engineering, University of Texas at San Antonio, San Antonio, TX, USA

Graduate Program in Biomedical Engineering, University of Texas Health Science Center at San Antonio, San Antonio, TX, USA
e-mail: solaleh.miar@utsa.edu; teja.guda@utsa.edu

A. Shafiee
Wake Forest Institute for Regenerative Medicine, Winston-Salem, NC, USA
e-mail: asnf2@mail.missouri.edu

R. Narayan (✉)
UNC/NCSU Joint Department of Biomedical Engineering, Raleigh, NC, USA

Diabetes Center for Research, Department of Biomedical Engineering, UNC School of Medicine, Chapel Hill, NC, USA
e-mail: roger_narayan@unc.edu

A. Ovsianikov et al. (eds.), *3D Printing and Biofabrication*, Reference Series in Biomedical Engineering, https://doi.org/10.1007/978-3-319-45444-3_2

Abstract

Additive manufacturing is becoming a focus of attention owing to its unique abilities to fabricate different objects using various materials. Perhaps printing technologies are the most popular type of additive manufacturing that is gaining ground in a wide range of industrial and academic utilization. Three- and two-dimensional printing of different materials such as ceramics, plastics, and metals as well as electronic functional materials is considered as the next revolution in science and technology. Importantly, these technologies are being used extensively in medical applications. Tissue engineering, which aims to fabricate human tissues and organs, is benefiting from the reproducible, computer-controlled, and precise procedure that can be obtained by printers. Three-dimensional printings of scaffolds, cell-laden biomaterials, and cellular (scaffold-free) materials hold a great promise to advance the tissue engineering field toward the fabrication of functional tissues and organs. Here, we review the utilization of different printing technologies for various tissue engineering applications. The application of printers in tissue engineering of bones, cartilages, and tendons and ligaments is di. Moreover, an overview of the advancements in printing skeletal muscles as well as the cardiovascular system is given. Finally, future directions and challenges will be described.

List of Abbreviations

ATST	Apparent tissue surface tension
AM	Additive manufacturing
ACL	Anterior cruciate ligament
CAD	Computer aided design
CADD	Computer aided design and drafting
DLP	Digital light processing
EBM	Electron beam melting
ECM	Extra cellular matrix
FDM	Fused deposition modeling
FFF	Fused filament fabrication
GAG	Glycosaminoglycan
HA	Hydroxyapatite
hPMSCs	Human placenta-derived mesenchymal stem cells
MHC	Myosin heavy chain
MSCs	Mesenchymal stem cells
PAM	Pressure-assisted microsyringe
PCL	Polycaprolactone
PED	Precision extrusion deposition
PEG	Polyethylene glycol
PEGDMA	Poly (ethylene glycol)dimethacrylate
PEO	Polyethylene oxide
PHBV	Poly (hydroxybutyrate-co-hydroxyvalerate)

PLA	Polylactic acid
PLDLLA	Poly (L-lactide-co-D,L-lactide)
PLGA	Poly-lactic-co-glycolic acid
PLLA	Poly (L-lactide) acid
PPF	Poly (propylene fumarate)
SEM	Scanning electron microscopy
SLA	Stereolithography
SLM	Selective laser melting
SLS	Selective laser sintering
TCP	Tricalcium phosphate
3D	Three-dimensional

1 Introduction

Synthetic scaffold grafts have traditionally been produced using various manufacturing processes, including mold casting; gas foaming; salt leaching; freeze drying; fiber fabrication from polymeric materials; powder metallurgy, forming, and stock machining for metallic biomaterials; and sintering for ceramic biomaterials. Shape, porosity, and interconnectivity are among the most important properties for the success of biomaterials in scaffolds or implants. However, conventional manufacturing processes cannot readily provide independent control over these structural properties. Additive manufacturing (AM) techniques, which were first introduced in 1986 by Charles Hull (Wohlers and Gornet 2014), have been actively embraced for accurate three-dimensional design and development of scaffold materials and implants. Since the first patent published by Hull's group describing stereolithography, various methods have been developed based on similar concepts to prepare highly organized three-dimensional structures. AM is based on the layer-by-layer synthesis of metals, polymers, ceramics, or their composites, with the manufacturing tolerance and resolution based on the thickness of the layer and the method of controlling material deposition within the layer. Various forms of material such as liquids, solids, or powders can be assembled using this approach. The bottom-up approach associated with AM lends itself to the creation of architectures that traditional manufacturing processes are limited in addressing such as internal porosities, lack of residual stress, and interlocking shapes without connections. Figure 1 shows a summary of various AM methods currently in development that are described in the recent literature (Standard 2012; Wong and Hernandez 2012; Thavornyutikarn et al. 2014). Moreover, AM has recently evolved from the layering of materials to the incorporation of cells during the AM process. This approach, known as bioprinting, has many advantages for tissue regeneration. This method was first reported by Thomas Boland and colleagues at Clemson University in 2003 (Doyle 2014).

Regardless of the different printing approaches, AM involves three main steps (Gibson et al. 2010). First, all designs are precisely prepared through 3D modeling software, which builds spatial image models (CAD, STL, SLI, CADD). The 3D images are corrected or modified. Models are processed by a slicer software to make

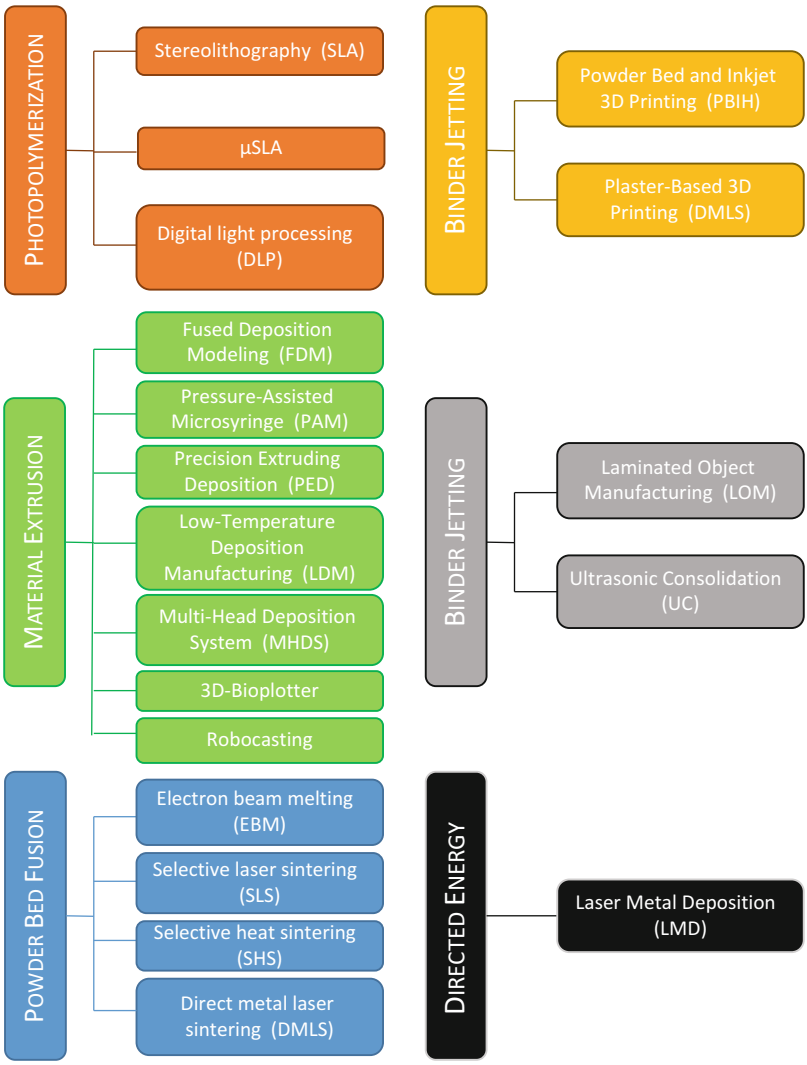

Fig. 1 Techniques utilized for AM of biomaterials

two-dimensional images for the next step (Kruth et al. 1998). The second step includes printing the model in a layer-by-layer manner using different materials or bioinks. The last step is related to curing, sintering, final finishing (Wong and Hernandez 2012), or other post-printing procedures (Kruth 1991). This step is highly dependent on the material. For example, bioprinted structures mostly require a post-printing step to evaluate the stability of the design and availability of sufficient nutrients (Murphy and Atala 2014). Ceramic or polymeric structures may require sintering (Travitzky et al.

2014) or post-polymerization processing (Wang et al. 2017) as well as inspection to validate the geometrical conformity to design tolerances.

The most important advantage of AM is the capability of the approach to produce customized structures, which constitute the prosthesis or scaffold. Modular implant manufacturing specially focuses on femoral (McCarthy et al. 1997; Geetha et al. 2009), wrist (Rahimtoola and Hubach 2004), and other small joint implants (Carignan et al. 1990). Although traditional mold casting and machining methods are time and cost-effective at an industrial scale, they are unable to provide customization tailored to individual patient needs. As a result, patients may face complications such as implant failure. It is anticipated that the next generation of modular implants will be based on accurate patient image data (Rengier et al. 2010; Bhumiratana and Vunjak-Novakovic 2012), in which each part can be customized before fabrication. Figure 2 shows a 3D-printed personalized titanium plate (Ma et al. 2017). Moreover, AM techniques allow for novel surface morphology features that can enhance cellular attachment and tissue infiltration. One such method is electron beam melting (EBM), in which materials are fused together by an electron beam in vacuum environment. EBM can be used for fabrication of

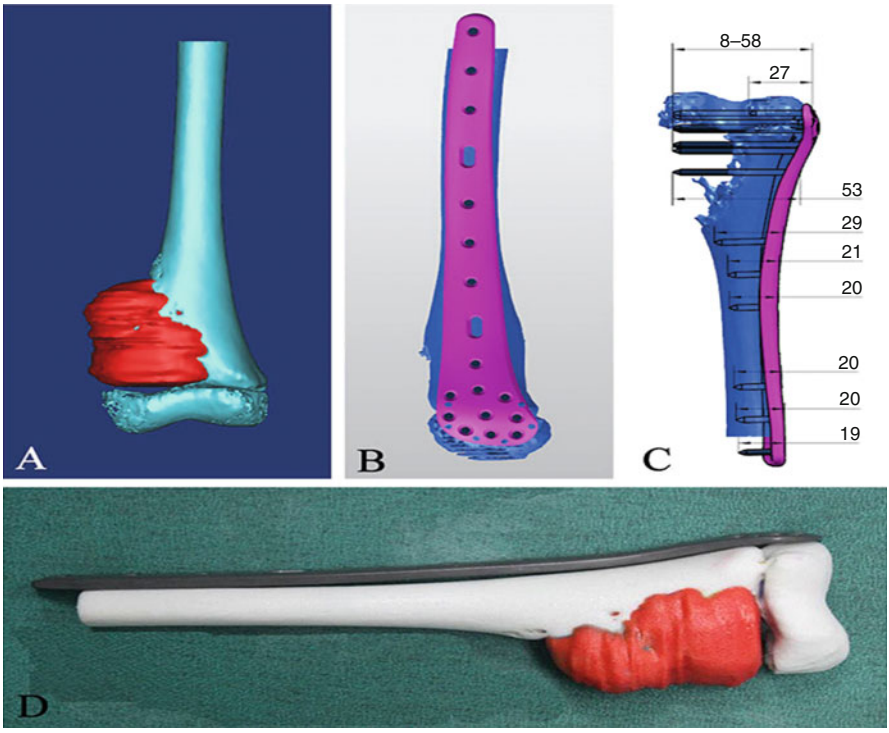

Fig. 2 3D-printed personalized titanium plates (Ma et al. 2017)

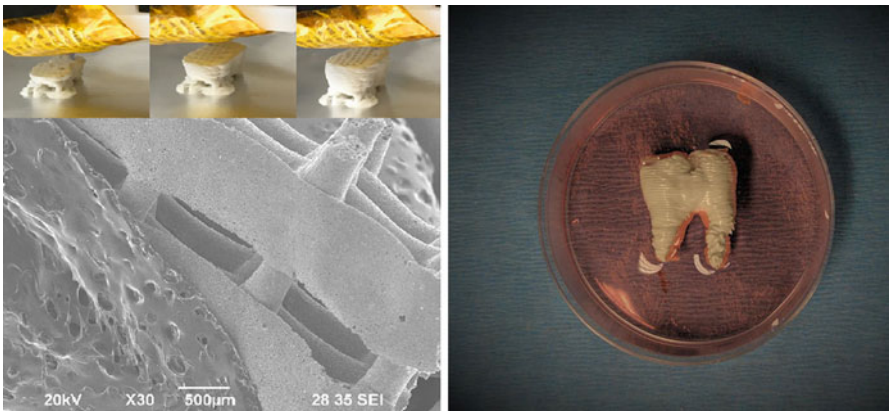

Fig. 3 Hydroxyapatite-based 3D tooth printed by Bioplotter

metallic meshes such as porous Ti6Al4V; the structures can contain surface features (Murr et al. 2010) for bone ingrowth and interfacial integration, enabling cement-free prostheses. Also, internal and external fixation devices including screws and plates have been printed based on patient 3D models (Qiao et al. 2015).

Beside implants, modular tissue engineering (Nichol and Khademhosseini 2009) offers customized fabrication for complex architectures such as the bone. Long bones are made of cancellous and compact bone in addition to the bone marrow and blood vessels (Melchels et al. 2012). However, conventional methods cannot readily produce structures with this complex morphology. AM, being a bottom-up process, has made it possible to produce integrated structures with different porosities, surface contours, and roughness values (Schantz et al. 2003; Naing et al. 2005; Zhang et al. 2008). Figure 3 is a personalized 3D structure of the teeth printed in our lab and an SEM picture of the printed layers.

Cartilage tissue, despite the characteristic low cell density and the absence of vascularization, continues to remain a challenge for tissue engineering. Early studies on the use of AM for cartilage tissue regeneration focused on acellular scaffold fabrication through extrusion-based methods (Hutmacher 2000; Schuurman et al. 2013). More recently, bioprinting methods have been employed to achieve uniform cell seeding and matrix organization through multi-head deposition systems (Kundu et al. 2015). Reports indicate that encapsulated cells, matrix, and proteins can be printed with independent spatial control to mimic the natural structure of the cartilage (Shim et al. 2012; Schuurman et al. 2013).

The skeletal muscle is a complex structure made of microfibers. Muscle contraction depends on actin and myosin filaments, which are stacked to form sarcomeres. As indicated by muscle regeneration studies, electrical (Rangarajan et al. 2014), mechanical (Rangarajan et al. 2014), and chemical (Husmann et al. 1996) factors lead to the differentiation of muscle cells. However, morphology and the scaffold design play prominent roles in the functionality of the muscle fibers. Studies show that aligned fibers facilitate the formation of aligned muscle cells (Aviss et al. 2010).

Although electrospun fibers have shown promise for muscle tissue regeneration, this technology is still limited to two-dimensional tissue culture. Bioprinting not only provides more accurate fibrous structures (Ker et al. 2011), but it also produces aligned and reproducible 3D patterns (Cvetkovic et al. 2014; Yeo et al. 2016; Costantini et al. 2017). Bioprinting has been successfully used in interfacial tissue regeneration, including the synthesis of tendon-muscle units (Weiß et al. 2011; Merceron et al. 2015); for example, a combination of two types of polymers (thermoplastic polyurethane and poly (ε-caprolactone)) along with C2C12 and 3 T3 cells were printed to form an interface region of a tendon-muscle unit.

One of the advantages of personalized designs is the ability of printing of grafts in situ (Ventola 2014). While in situ bioprinting has been conducted for the treatment of skin lesions (Ozbolat and Yu 2013), it is anticipated that handheld bioprinters for in situ printing will facilitate graft or implant customization (Cui et al. 2012a) and will provide an additional tool for reconstructive surgeons.

Here we overview the application of additive manufacturing in some aspects of tissue engineering such as the bone, cartilage, muscle, tendon, and ligament, as well as cardiovascular research.

2 Bone

Successful new bone formation requires ECM formation, functional vascularization, and proper innervation. Synthetic grafts that meet these criteria are best designed in a modular fashion with an organized spatial design. AM enables the fabrication of structures with tailored microlevel porosity and the design of cell-free scaffolds by precise 3D deposition of metals (Bobbert et al. 2017) and ceramics (Bose et al. 2003; Leukers et al. 2005).

The preferred techniques for manufacturing ceramic-based scaffolds include powder bed fusion, binder jetting, and extrusion-based methods. Powder bed fusion is the method of choice when the stock material is available in powder form and works with both ceramic (Shuai et al. 2013) and polymer powders. Binder jetting, which is a hybrid of powder bed and ink-jet printing approaches, deposits binding agent on specified places of the substrate covered with powder particles. Binder jetting is an ideal technique to fabricate ceramic-based bone grafts made of silica and zinc oxide (Fielding et al. 2012), tricalcium phosphate (TCP) (Gbureck et al. 2007a, b; Tarafder et al. 2013b), and hydroxyapatite (HA) (Seitz et al. 2005; Igawa et al. 2006). Another fabrication technique in this family involves the use of a selective laser sintering (SLS) (Duan et al. 2010) that sinters designed places on a substrate covered with powder. Moreover, a frequently employed extrusion-based technique is robocasting. This method has been used to process HA (Dellinger et al. 2007; Miranda et al. 2008; Fu et al. 2011), TCP (Martínez-Vázquez et al. 2010), Bioglass (Fu et al. 2011), and their composites containing polymers such as polylactic acid (PLA) (Russias et al. 2007) and PCL (Heo et al. 2009).

Systems comprising solely of polymers have also been widely investigated for bone graft fabrication. Among biocompatible polymers, polycaprolactone (PCL) has

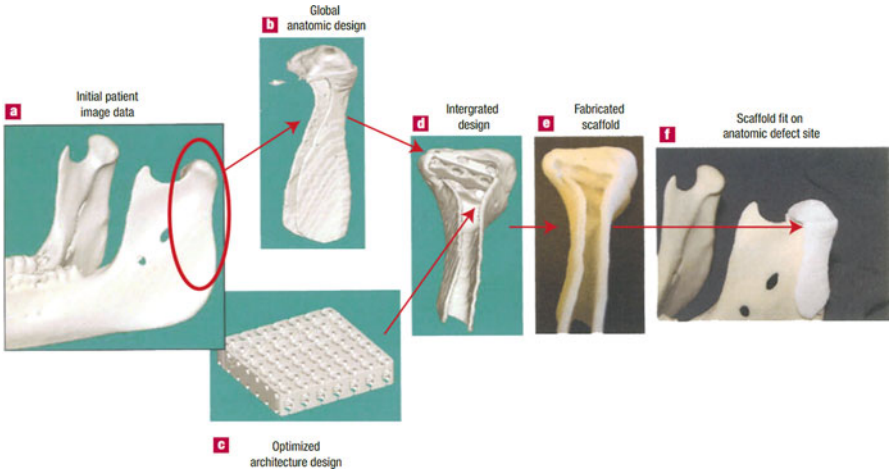

Fig. 4 Customized porous scaffold made through solid free-form fabrication and selective laser sintering. (Hollister 2005)

been used in bone scaffolds due to its mechanical properties, which are similar those of the bone (Oh et al. 2007). Its composites with ceramics, including HA or TCP (Hoque et al. 2012), have been frequently modeled by rapid prototyping and fabricated by extrusion-based printing. Poly-lactic-co-glycolic acid (PLGA) (Ge et al. 2009) and poly (L-lactide-co-D,L-lactide) (PLDLLA) (Lam et al. 2009a) can be processed into bone grafts using extrusion and powder printing. Powder printing is also ideal for ceramics-based scaffolds that require an appropriate binder. Binders affect the mechanical properties of the green (unsintered) part and hence determine the success of the final product. Various categories of binders have been optimized for particulate suspension and print cohesiveness, including water-based (Suwanprateeb and Chumnanklang 2006), organic (Vorndran et al. 2008; Suwanprateeb et al. 2012), and starch-based binders that are suitable for bone scaffold fabrication (Bose et al. 2013). Figure 4 shows a personalized scaffold made of PCL. This scaffold was designed by solid free-form fabrication and printed using SLS (Hollister 2005).

Direct writing is another extrusion-based method to produce polymer scaffolds (Serra et al. 2013). The advantage of this method is that it can be conducted at low temperature; therefore, growth factors and other temperature-sensitive agents can be safely loaded into the ink (Seyednejad et al. 2012). Some natural polymers such as alginate (Luo et al. 2015), gelatin (Zhang et al. 2013), and collagen (Kim and Kim 2013) have been used in bone scaffolds that are produced by this method. This method is based on the same principle as low-temperature deposition (Xiong et al. 2002), namely, direct layer-by-layer assembly of the material. This technique requires solvent compatibility for all of the system components, including one or more polymers, growth factors, or ceramic powders (Kim and Cho 2009; Liu et al. 2009). The other approach in extrusion-based methods is fused filament fabrication

(FFF) based on material melting for extrusion through the printer nozzle (Kalita et al. 2003; Ramanath et al. 2008). The limitation of this method is the high temperature required for melting the polymers, which prevents incorporation of drugs and biologics. Pressure-assisted microsyringe (PAM), precision extruding deposition (PED), and plotting are the other extrusion-based techniques that are used for polymeric bone scaffolds. PAM includes a reservoir with a capillary needle filled with polymer solution. The materials are printed using controlled air pressure. PCL (Vozzi et al. 2002), poly (L-lactide) acid (PLLA) (Vozzi et al. 2002), PLGA (Vozzi et al. 2003), and polyurethane (Tartarisco et al. 2009) are the polymers that are typically processed using the PAM method. PCL (Wang et al. 2004; Khalil et al. 2005; Shor et al. 2005; Shor et al. 2009) scaffolds have also been synthesized using PED. In this technique scaffold materials can be used in a granulated form, and filament preparation is not necessary. In addition to pure PCL, composite inks with alginate (Khalil et al. 2005) and HA (Shor et al. 2005) have also been prepared. Plotters are the other category of extrusion-based AM techniques, with PCL (Sobral et al. 2011) and starch (Oliveira et al. 2009; Oliveira et al. 2012) being the most conducive materials for ink formulation.

Selective laser sintering (SLS) and stereolithography (SLA) are other techniques that require photopolymerization to solidify the scaffold. SLS can involve the use of polymer powder to sinter structures for the preparation of bone scaffolds. One of the most commonly used polymers is poly (hydroxybutyrate-co-hydroxyvalerate) (PHBV) (Pereira et al. 2012) and its composites with other polymers such as PLLA (Duan et al. 2010) and ceramics such as calcium phosphate (Duan and Wang 2010a; Duan et al. 2010). In addition, PCL scaffolds made via SLS were able to incorporate an orthogonally porous structure for load-bearing sites, which optimized porosity and structural strength (Eshraghi and Das 2010; Thavornyutikarn et al. 2014). SLA uses photopolymerization to make layer by layer a 3D object. Among SLA methods, both μSLA and digital light processing (DLP) offer higher resolution and have been used to manufacture scaffolds for bone tissue regeneration (Thavornyutikarn et al. 2014). Materials used in these studies include poly (propylene fumarate) (PPF) (Choi et al. 2009) and PCL-infiltrated ceramic scaffolds (Seol et al. 2013), with pore sizes ranging from 100 μm to 300 μm; these scaffolds have shown efficacy in supporting both the bone and associated vascular ingrowth.

In addition to accurate morphology and controlled porosity, the mechanical properties of bone scaffolds are the most important parameters that are evaluated for 3D-printed scaffolds. Similar to ceramic scaffold synthesis, the crucial post-printing step is sintering, which is required to reinforce the structure by the reformation of grain domains in the green body; this approach results in significantly greater strength and toughness that are essential parameters to fabricate tissues such as the bones. One of the new methods is microwave sintering, which has gained favor over conventional sintering since it offers lower energy consumption, reduced sintering time, better grain distribution, and improved mechanical properties (Oghbaei and Mirzaee 2010). For example, microwave-sintered TCP scaffolds fabricated by direct 3D printing showed an increase in compressive strength of up to 69% (Tarafder et al. 2013a) in comparison to the conventional sintered material. In

addition, other new methods (Bose et al. 2013) such as bioactive liquid phase sintering have been used to sinter hydroxyapatite/apatite-wollastonite glass composites fabricated by the 3D printing method, which improved the green strength of the composite from 1.27 MPa to 76.82 MPa (Suwanprateeb et al. 2009). A recent method (Khalyfa et al. 2007; Bose et al. 2013) to preform composite green structures has involved the immersion of HA or TCP scaffolds in monomers before sintering. In one report, scaffolds were immersed in copolymers such as PLLA and PCL to improve the mechanical properties via infiltration (Lam et al. 2002). More recently, this approach has also been used to improve the flexural strength of ceramic composites. In these studies, HA scaffolds exhibited an increase in bending modulus and strength by using infiltration after printing (Suwanprateeb et al. 2008).

Post-processing of metallic 3D-printed scaffolds is limited to final finishing; however, finishing may not be necessary due to the accuracy of the printed microstructure (Hedayati et al. 2017). Metallic scaffolds are mostly printed by selective laser melting (SLM) (van Hengel et al. 2017), EBM (Murr et al. 2012; Bsat et al. 2015; Zadpoor and Malda 2017), and SLS (Traini et al. 2008). All of these methods are based on one single sintering source at a powder bed. Recently, a new method called laser engineering net shaping has proposed powder injection in conjunction with the laser source as opposed to powder in bed (Atala and Yoo 2015). Of the methods noted, SLM is not limited to metals alone; polymer-ceramic composites have also been fabricated using this technique (Duan et al. 2010).

While 3D printing has largely been for the synthesis of cell-free scaffolds, bioinks (Ahn et al. 2012) containing various cell types and biomolecules along with polymers or ceramics have been investigated to expand the potential application of AM systems for regenerative medicine. Toxic solvents, high temperatures, and strong UV exposure are incompatible with cells, necessitating a substantive change from traditional 3D printing approaches to enable AM of biologics. Therefore, the selection of materials and systems for bioprinting-based graft fabrication is limited. Ink-jet bioprinting (Samad et al. 2011; Gao et al. 2014), extrusion bioprinting (Poldervaart et al. 2013), and stereolithographic bioprinting (Zhou et al. 2016) are methods that are frequently used for the preparation of cell-laden 3D structures. Cell suspensions containing alginate (Ahn et al. 2013), polyethylene glycol (PEG) (Gao et al. 2015a), and poly (ethylene glycol)dimethacrylate (PEGDMA) with bioactive glass and HA nanoparticles (Gao et al. 2014) have been utilized in bioprinting studies. One of the new techniques, which was first attempted for skin tissue regeneration, is laser printing (Koch et al. 2012); this approach provides a new mechanism for generating multicellular 3D designs with potential use in bone regeneration (Gruene et al. 2010). Moreover, bioprinting methods allow growth factors and other biomolecules to be directly incorporated (potentially in the same locations as the target cells) and locally released. Growth factors such as fibroblast growth factor (Ker et al. 2011), vascular endothelial growth factor (Poldervaart et al. 2014), and bone morphogenetic proteins (Poldervaart et al. 2013) have incorporated within bioprinted scaffolds; localized release from bioprinted scaffolds and release profiles have been reported. Table 1 (I–XI) discusses studies related to the use of AM in bone tissue regeneration.

Table 1 Various AM techniques used in bone tissue regeneration

Publication	Material (s)	Cell type (s)	Porosity (%)	Pore size (μm)	Strength (MPa)
I. Vat photopolymerization – Stereolithography					
(Cooke et al. 2003)	Diethyl fumarate (DEF), poly (propylene fumarate) (PPF)	–	90	150–800	20–70
(lee et al. 2007b)	Poly (propylene fumarate)	–	61–63	600–1000	11–146
(Padilla et al. 2007)	Bioactive glass	–	–	400, 1400	–
(Bian et al. 2011)	β-TCP and acrylamide, methylenebisacrylamide	–	45	600–800	24
(Tesavibul et al. 2012)	Bioglass	–	50	500	0.33
(Ronca et al. 2013)	Poly (d,l-lactide)/nano-sized hydroxyapatite (PDLLA/ nano-hap) composite resin	–	63–66	620–690	50–66
(Barry et al. 2008)	OCM-2	HOBS	40	–	–
(Jansen et al. 2009)	Fumaric acid monoethyl ester-functionalized poly (D, L-lactide)/ N-vinyl-2-pyrrolidone resins	MC3T3	76	260	0.01–2.1
(Melchels et al. 2009)	Poly (d,l-lactide)	MC3T3	83	170–240	
(Heller et al. 2009)	Vinyl ester	MC3T3-E1	–	–	1.5–1.7
(Lan et al. 2009)	Poly (propylene fumarate) (PPF)	MC3T3-E1 pre-osteoblasts	65	250	68.8 ± 9.4
(Melchels et al. 2010)	PDLLA	A4–4	70	255	–

(*continued*)

Table 1 (continued)

Publication	Material (s)	Cell type (s)	Porosity (%)	Pore size (μm)	Strength (MPa)
(Seck et al. 2010)	Poly (ethylene glycol)/poly (d,l-lactide)-based resins	hMSC	52	423	–
(Lee et al. 2011)	PLGA	MC3T3-E1 pre-osteoblasts	69.6	430	–
(Elomaa et al. 2011)	Poly (ε-caprolactone)	NIH3T3 fibroblasts	69–71	465	–
(Seol et al. 2013)	HA and TCP powder	hTMSCs	–	300	2.47 ± 0.035
(Elomaa et al. 2013)	Bioactive glass and photocrosslinkable poly (ε-caprolactone)	Human gingival fibroblasts	77	476–594	~2.5
II. Vat photopolymerization – Two-photon printing					
(Claeyssens et al. 2009)	Biodegradable triblock copolymer poly (ε-caprolactone-co-trimethylenecarbonate)-b-poly (ethylene glycol)-b-poly (ε-caprolactoneco-trimethylenecarbonate)	Only cytotoxicity texts: Murine fibroblast cell line NIH-3 T3	–	–	96 ± 2 kPa
(Petrochenko et al. 2015)	Biodegradable urethane and acrylate-based photoelastomer	Human bone marrow stem cells	60	200	–
(Marino et al. 2014)	Hybrid photoresist (Ormocomp®)	SaOS-2 bone-like cells	–	–	–
III. Vat photopolymerization – Digital light processing					
(Dean et al. 2012)	PPF	–	–	800	–

(Tesavibul et al. 2012)	45S5 Bioglass	–	50	500	–
(Lee et al. 2012)	PCL and PLGA	Mouse osteoblastic cell line MC3T3-E1	57.2	200	6.05–9.81
IV. Vat photopolymerization – uSLA					
(Lu et al. 2006)	PEGDA	Murine OP-9 marrow stromal cells	–	165–650	–
(Kim et al. 2007)	HA	NA	–	250	–
(Lan et al. 2009)	PPF/diethyl fumarate (DEF)	MC3T3-E1 pre-osteoblast	65	250	–
(Lee et al. 2009)	PPF/DEF-HA	MC3T3-E1 pre-osteoblasts	–	430	–
(Lee et al. 2011)	Poly (propylene fumarate)/ diethyl fumarate photopolymer loaded PLGA microspheres	MC3T3-E1 pre-osteoblasts	69.6	430	–
(Seol et al. 2013)	Ha-TCP- PCL	Human turbinate mesenchymal stromal cells (hTMSCs)	–	300	–
(Raman et al. 2016)	Poly (ethylene glycol) dimethacrylate (PEG-dma) resin	Murine cells (fibroblasts, myoblasts, endothelial, and bone marrow stromal cells	–	100	–
(Owen et al. 2016)	Polymerized high internal phase emulsions	Embryonic stem cell-derived mesenchymal progenitor cells (hES-MPs)	–	300 μm (vertically) and 650 μm (laterally)	UTS from 2.03 to 0.11
(Mott et al. 2016)	Poly (propylene fumarate) (PPF)	L929 cell	–	–	7.8–36.5

(*continued*)

Table 1 (continued)

Publication	Material (s)	Cell type (s)	Porosity (%)	Pore size (μm)	Strength (MPa)
V. Material extrusion – Robocasting					
(Miranda et al. 2006)	β-Tricalcium phosphate	–	45	75	20
(Russias et al. 2007)	HA and bioglass with PLA and PCL as the ink	–	75	200–500	–
(Dellinger et al. 2007)	Hydroxyapatite	–	–	100–600	–
Martínez-Vázquez	β-tricalcium phosphate polylactic acid (PLA) and poly (ε-caprolactone) (PCL)	–	25	–	20–130
(Fu et al. 2011)	Bioactive glass	–	60	500	136 ± 22
(Heo et al. 2009)	m-HA/PCL	MG-63 osteoblast-like cells	72–73	500	–
(Serra et al. 2013)	PEG	Rat mesenchymal stem cells	85.7–87.2	375 ± 25	–
(Keriquel et al. 2010)	Nano-hydroxyapatite (n-HA)	In vivo	–	–	–
VI. Material extrusion – Fused deposition modeling (FDM)					
(Lam et al. 2007)	β-TCP and PCL	–	68	–	–
(Lam et al. 2008)	β-TCP and PCL	–	69	–	–
(lam et al. 2009b)	β-TCP and PCL	–	70	–	–
(Ramanath et al. 2008)	Poly-ε-caprolactone	–	–	–	–
(Martins et al. 2009)	Starch and polycaprolactone	–	68.3–79.4	–	–

(Iam et al. 2009a)	PLDLLA/TCP	–	–	–	23
(Tellis et al. 2008)	Polybutylene terephthalate	–	57–79	196–292 and 120–772	–
(Hutmacher et al. 2001)	PCL	Fibroblast and osteoprogenitor cell	61	–	3.1
(Darsell et al. 2003)	Alumina	OPC1	29–44	300	130–70
(Kalita et al. 2003)	Polypropylene (PP) polymer and tricalcium phosphate (TCP)	OPC1	36–52	160	12.7
(Zhou et al. 2007)	Polycaprolactone and polycaprolactone-tricalcium phosphate	Alveolar bone	43–65	–	x-axis, 2.2, 4.4; z-axis, 1.5–3.1
(Shor et al. 2007)	Polycaprolactone/ hydroxyapatite	Primary fetal bovine osteoblast	60–70	450	–
(Ye et al. 2010)	PCL	MG63 cells	53–76	400–500	2.7–7.9
(Korpela et al. 2013)	Poly (ε-caprolactone)/ bioactive glass	Fibroblast	30–40	400	–
VII. Material extrusion – Precision extruding deposition (PED)					
(Xiong et al. 2001)	PLLA	–	60.3	500 × 400	8.32
(Wang et al. 2004)	PCL	–	–	200–300	–
(Shor et al. 2005)	Polycaprolactone (PCL)/ hydroxyapatite (HA)	Endothelial cells (RHEC)	64	400	–
(Khalil et al. 2005)	PCL-alginate	Human endothelial cells	–	650	–
(Shor et al. 2009)	Polycaprolactone	Primary fetal bovine osteoblast cells	65	350	5.3

(*continued*)

Table 1 (continued)

Publication	Material (s)	Cell type (s)	Porosity (%)	Pore size (μm)	Strength (MPa)
(Yildirim et al. 2010)	PCL	7F2 mouse osteoblast cells	–	300	–
VIII. Material extrusion – Low-temperature deposition manufacturing (LDM)					
(Xiong et al. 2002)	Poly (l-lactic acid) (PLLA), tricalcium phosphate (TCP)	–	89.6	400	Bend strength, 12.1; compressive yield strength, 4.71
(Liu et al. 2009)	PLGA, collagen, gelatin, chitosan, TCP	–	–	300–500	–
(Li et al. 2011)	PLGA- TCP	HBMSCs	87.4	380	–
(Hsu et al. 2012)	Chitosan	MC3T3-E1	–	From the top view 500 × 500	–
(Park et al. 2011)	Poly (lactic-co-glycolic acid) grafted hyaluronic acid	In vivo, in vitro release of bmp2	–	250–300	–
IX. Material extrusion – Bioplotter and 3D plotter					
(Oliveira et al. 2009)	Starch/polycaprolactone	–	–	–	–
(Sobral et al. 2011)	Poly (ε-caprolactone)	Human osteosarcoma cell line SaOs-2	10–85	100–900	
(Oliveira et al. 2012)	Starch/poly-e-caprolactone (SPCL)	Bone marrow mesenchymal stem cells	70	–	–
(Lode et al. 2014)	Paste-like CPC	hMSCs	56	–	6.1 ± 1.8
X. Powder bed fusion – Electron beam melting (EBM)					
(Thomsen et al. 2009)	Ti6Al4V	–	–	–	910–940
(Heinl et al. 2008)	Ti6Al4V	–	59.5–81.1	1230	Diamond structure, 16.1–22 Mpa; hatched structure, 49.6–107.5 Mpa

(Li et al. 2009)	Ti6Al4V	–	66.3	1108	67.7
(Parthasarathy et al. 2010)	Ti6Al4V	–	60.91–74	1000–1230	7.28–163.02
(Murr et al. 2011)	Ti6Al4V	–	–	400	–
(Cheng et al. 2012)	Ti6Al4V	–	62.08–91.65	–	3.8–112.8
(Campoli et al. 2013)	Ti6Al4V	–	10–20	–	–
(Ahmadi et al. 2014)	Ti6Al4V	–	–	–	–
(Zhao et al. 2016)	Ti6Al4V	–	62.1–64.5	30–80	61–196
(lv et al. 2015a)	Ti6Al4V	hMSCs	–	640	–
(lv et al. 2015b)	Ti6Al4V	Rat bone marrow-derived mesenchymal stem cells (rMSCs)	73–81.9	640–1200	–
(Ponader et al. 2010)	Ti6Al4V	In vivo	61.3	450	127.1–148.4
(Palmquist et al. 2013)	Ti6Al4V	In vivo	65–70	500–700	–
(Biemond et al. 2013)	Ti6Al4V	In vivo	49–63	250–800	2.0–3.2
(Wu et al. 2013)	Ti6Al4V	In vivo	68	710	63–120
XI. Powder bed fusion – Selective laser sintering (SLS)					
(Lorrison et al. 2005)	Glass-ceramic and a combination of hydroxyapatite and phosphate glass	–	–	–	–

(*continued*)

Table 1 (continued)

Publication	Material (s)	Cell type (s)	Porosity (%)	Pore size (μm)	Strength (MPa)
(Simpson et al. 2008)	Poly (L-lactide -co-glycolide)	–	125–250	46.5	12.06 ± 2.53
(Eosoly et al. 2010)	Hydroxyapatite/ poly-ε-caprolactone	–	–	1200	0.1 and 0.6
(Duan and Wang 2010b)	Ca–P/PHBV	–	1.0 × 1.0 × 1.0 mm3	–	–
(Kolan et al. 2012)	13–93 bioactive glass	–	50	300–800	41–157
(Pereira et al. 2012)	Poly (3-hydroxybutyrate) (PHB)	–	–	–	–
(Shuai et al. 2013)	β-tricalcium phosphate	–	–	600	–
Dadbakhsh et al. 2014)	NiTi	–	–	–	–
(Wiria et al. 2007)	PCL/HA biocomposite	105	–	–	2.53–11.54
(Zhang et al. 2009)	HA-PE and HA-filled PA	HOB cells	10–100	46–47	–
(Kanczler et al. 2009)	PLA	Human fetal femur-derived cells	–	–	–
(Duan and Wang 2010a)	Ca–P/PHBV	Human osteoblast-like	800	64.6 ± 2.0 – 62.6 ± 1.2	–
(Duan et al. 2010)	Calcium phosphate (ca-P)/ poly (hydroxybutyrate-co-hydroxyvalerate) (PHBV) and carbonated hydroxyapatite (CHAp)/poly (l-lactic acid) (PLLA) nanocomposite microspheres	Human osteoblast-like cell line (SaOS-2)	62–70	800	0.47–0.63

(Sudarmadji et al. 2011)	PCL	Osteoblasts	–	40–80	0.17–5.03 MPa
(Eosoly et al. 2012)	Polycaprolactone-hydroxyapatite	MC 3 T3	–	1200	0.15–0.41
(Van Bael et al. 2013)	PCL	hPDC	1500–2000	–	0.97 ± 0.03
(Williams et al. 2005)	Polycaprolactone	Primary human gingival fibroblasts	1750–2500	17.8–55	2.0–3.2 Mpa
(Goodridge et al. 2007)	A–M glass-ceramic and 45S5	In vivo	–	–	–
(Lohfeld et al. 2012)	Polycaprolactone/tricalcium phosphate	In vivo	51–77	Up to 1000	–
XII. Powder bed fusion – Selective heat sintering (SHS)					
(Tosun et al. 2009)	NiTi	–	–	50.7–59.7	–
(Tosun and Tosun 2012)	NiTi	–	–	50.3–57.4	–
(Tosun et al. 2012)	NiTi	–	205.98–741.35	–	–
(Resnina et al. 2013)	NiTi	–	Preheating temperature of 613 for Ti, 48.0 at.% Ni; Ti, 50.0 at.% Ni mixture; 653 K for Ti, 45.0 at.% Ni; Ti, 52.0 at.% Ni mixture, 180–349; preheating temperature of 723 for Ti, 45.0 at.% Ni; Ti, 52.0 at.% Ni mixture; 773 K for Ti, 48.0 at.% Ni; Ti, 50.0 at.% Ni mixture, 220–363	54–66	–

(*continued*)

Table 1 (continued)

Publication	Material (s)	Cell type (s)	Porosity (%)	Pore size (μm)	Strength (MPa)
(Shishkovsky et al. 2010)	NiTi	In vivo	–	40–50	–
XIII. Powder bed fusion – Direct metal laser sintering (DMLS)					
(Bertol et al. 2010)	Ti6Al4V	–	–	–	–
(Jardini et al. 2011)	Ti6Al4V	–	–	–	–
(Barucca et al. 2015)	Co–Cr–Mo	–	–	–	–
(Ciocca et al. 2011)	Titanium	In vivo	–	–	–
(Stübinger et al. 2013)	Titanium	In vivo	–	500	–
XIV. Binder jetting – Powder bed and ink-jet 3D printing (PBIH)					
(Gbureck et al. 2007)	Calcium phosphate and PLA/PGA polymer solutions	–	HA, 12 um; dicalcium phosphate dihydrate, 13 um	Brushite ceramics, 29–45 and hydroxyapatite ceramics, 55–60	DCPD, 22.3; HA, 5.8
(Klammert et al. 2010)	TCP	–	–	28–35	Bending strength: 3.9–5.2
(Winkel et al. 2012)	Bioactive glass and hydroxyapatite	–	900–2000	–	70
(Suwanprateeb et al. 2012)	HDPE	–	132.6–136.2	22.3–49.7	4
(Seitz et al. 2005)	Hydroxyapatite	Bone patient's cells	565	–	22
(Khalyfa et al. 2007)	TCP	MC3T3-E1	–	38	0.59–0.7

(Ge et al. 2009)	Poly-lactic-co-glycolic acid	Human fetal osteoblasts	1000	50	7.8
(Cooper et al. 2010)	DermaMatrix	C2C12	–	–	–
(Wiria et al. 2010)	Titanium powder	L-929 fibroblast cells	–	–	167–455
(Fielding et al. 2012)	Silicon dioxide and zinc oxide and synthetic β-tricalcium phosphate	Human fetal osteoblast	343.7–698	–	4.34–10.21
(Tarafder et al. 2013a)	β-TCP	Human fetal osteoblast cells (hFOB)	500–1000	42–63	10.95–6.6
(Santos et al. 2012)	TCP	Human osteoblast cell culture	30	46.07–54.44	2.36–8.66
(Xu et al. 2013b)	Alginate	dSMCs-bECs-hAFSCs	–	–	2.2
(Gao et al. 2014)	PEGDMA and ha	hMSCs and mesenchymal stem cell	–	–	–
(Gao et al. 2015a)	PEG-GelMA	hMSCs	–	–	30–63 Kpa
(Igawa et al. 2006)	HA and TCP powder	In vivo	–	55	Bending strength, 9; compressive strength, 20
(Gbureck et al. 2007)	TTCP	In vivo	HA, 12 um; dicalcium phosphate dihydrate, 13 um	Brushite ceramics, 29–45 and hydroxyapatite ceramics, 55–60	DCPD, 22.3; HA, 5.8
(Saijo et al. 2009)	TCP	In vivo	–	–	–
(Tarafder et al. 2013b)	β-TCP SrO and MgO	In vivo	245–311	27–35	12

3 Cartilage

Restoration of osteochondral tissue damaged due to age, degeneration, or injury is a significant concern in orthopedic health care. When therapies such as autologous chondrocyte transplantation and microfracture surgery are not feasible, cartilage tissue engineering is one of the potential options for articular surface regeneration (Hutmacher 2000; Temenoff and Mikos 2000). Different methods have been developed to design a non-vascularized structure for cartilages with similar mechanical properties to native tissue and an appropriate interface with bone tissue for functional load transfer and shear resistance. Various methods such as solution casting (Freed et al. 1993), freeze drying (Tan et al. 2009), phase separation (Mikos and Temenoff 2000), and fiber fabrication (Hutmacher 2000) have been previously examined; however, there is an absence of precise control over porosity and interconnectivity, which is necessary for successful bone growth at the interface. AM is a promising alternative for cartilage regeneration since it enables precise control over pore morphology as well as bulk structure. It also provides an opportunity to include different cell types (Sharma and Elisseeff 2004) during the manufacturing process, which was hitherto impossible using conventional methods due to the harsh environment associated with scaffold fabrication (e.g., high temperature or the presence of harmful solvents).

Additive manufacturing techniques such as stereolithography and methods combining techniques such as ink-jet printing, extrusion-based methods, and powder bed fusion have been successfully employed for cartilage scaffold processing (Santos et al. 2013; Vaezi et al. 2013). Due to the high cellularity of the tissue as well as given the lack of tissue vasculature, AM techniques for cartilage scaffold fabrication have focused to a greater extent on cell printing (Cui et al. 2012b; Di Bella et al. 2015) to enhance cellular delivery to the scaffold interior than methods for bone graft manufacturing.

The use of stereolithography for chondrogenic applications has been reported with a variety of polymers, including poly (trimethylene carbonate)-based resins (Schüller-Ravoo et al. 2013), Fumaric acid monoethyl ester (Jansen et al. 2009), PCL (Elomaa et al. 2011), (PDLLA-PEG)/hyaluronic acid (Sun et al. 2015), and polyacrylamide (Linzhong et al. 2010). Modified SLA techniques such as two-photon polymerization (Weiß et al. 2009), μSLA (Lee et al. 2007a, 2008; Weiß et al. 2011), and digital light processing (Sun et al. 2015) have been utilized to enhance the accuracy of scaffold fabrication for articular cartilage applications. Studies using SLA have so far been limited to biocompatibility and cell proliferation testing. A greater focus on tissue morphogenesis in long-term bioreactor culture or testing in appropriate translational preclinical models is necessary for further therapeutic advances in this area (Santos et al. 2013).

Ink-jet printing technology (Boland et al. 2006; Samad et al. 2010a, b, c) is a method based on the deposition of the polymeric ink in a drop-by-drop manner (Shafiee et al. 2008); this approach is able to form a line similar to those formed by filament extrusion-based systems. Using this technique, the researchers can deposit sub-microliter of materials on precise location of a substrate that reduces the

deposition cost dramatically by minimizing of material waste (Shafiee et al. 2009). An additive pattern containing such lines can be used to construct a 3D structure. This method has been used to create osteochondral scaffolds with different polymers and hydrogels; for example, PLGA-PLA is used in the cartilaginous zone, and PLGA-TCP is used at the transition associated with the cartilage-bone interface (Sherwood et al. 2002). In a study by Sherwood et al., the structural porosity and materials are designed to trigger chondrocyte proliferation and hypertrophy in the PLGA-PLA portion and simultaneously stimulate bone growth in the PLGA-TCP zone. There have also been studies related to the use of this approach for bioprinting. In one study, human chondrocytes were suspended in PEGDA and polymerized photochemically (Cui et al. 2014) to create a bioprinted cartilage gel. A modified version of the polymer (PEGDMA) has been reported for use in chondrocyte bioprinting. The design showed firm attachment of the printed structure to the surrounding tissue and greater proteoglycan deposition at the interface of the scaffold and the native cartilage (Cui et al. 2012b; Gao et al. 2015b), indicating local biocompatibility and cellular migration. In a similar study, it was demonstrated that bioprinted samples treated with growth factors showed chondrogenic properties due to the synergistic action of basic fibroblast growth factor and transforming growth factor beta-1 (Cui et al. 2012c). Other approaches have combined electrospinning with ink-jet printing to fabricate 3D hybrid structures containing electrospun PCL fibers and chondrocytes suspended in a fibrin-collagen hydrogel; this approach has provided an improvement in biological and mechanical properties (Xu et al. 2012).

The use of extrusion techniques and fused deposition modeling (FDM)-based methods to process polymers such as PCL alongside cells and growth factors is limited due to the high temperature (Cao et al. 2003; Hsu et al. 2007) required for polymer extrusion. FDM uses a continuous filament of material that can be melted using a high-temperature heater – the melted filaments fuse and solidify once it is dispensed from the nozzle. Poly (ethylene glycol)-terephthalate-poly (butylene terephthalate) (PEGT/PBT) block copolymer scaffolds have been developed using a modified FDM method that involves a fiber deposition technique (Woodfield et al. 2004). In another study, poly (ethylene oxide-terephthalate)-co-poly (butylene terephthalate) (PEOT/PBT) hollow fibers were extruded to form 3D scaffolds with the potential for controlled growth factor release (Moroni et al. 2006). Using the FDM method, 3D scaffolds were produced using PLGA and were modified post-printing with type II collagen for enhanced chondrocyte compatibility (Yen et al. 2009). It was found that increased fiber spacing in FDM scaffolds led to improved transport of degradation by-products, which limited the influence of the local acidic milieu on tissue regeneration. Liquid-frozen deposition manufacturing (LFDM) is another extrusion-based method that has been used to fabricate PLGA scaffolds. A direct head-to-head comparison between PLGA scaffolds manufactured by FDM and those manufactured by LFDM showed that LFDM scaffolds supported better chondrocyte proliferation and secreted extracellular matrix; FDM scaffolds showed lower cell numbers and matrix production because of heavy swelling (Yen et al. 2008). The LFDM method has been utilized to generate PLGA scaffolds that were loaded with

human placenta-derived mesenchymal stem cells (hPMSCs), which promoted the secretion of glycosaminoglycan (GAG) at twice the rate of mesenchymal stem cells (MSCs) (Hsu et al. 2011) and indicated an ability to support cartilage regeneration. Biodegradable polyurethane elastomers were also synthesized using LFDM in the form of nanoparticles, which were combined with polyethylene oxide (PEO); PEO served as a viscosity enhancer. This material was prepared as a scaffold and compared to PLGA using an in vitro chondrocyte cell seeding study, which demonstrated that cell proliferation and GAG secretion were higher in the PU scaffold than in the PLGA scaffold (Hung et al. 2014). These studies indicate that significant biomaterials optimization research needs to be conducted to identify the chemical and structural parameters that influence the promotion of a pro-chondrogenic niche. Such studies are essential for the further translation of LFDM-processed 3D structures for cartilage tissue engineering.

Cell-laden scaffolds have also been prepared using PLGA/alginate and PLGA-HA containing human fetal-derived stem cells and cartilage-derived ECM, which showed successful cartilage and subchondral layer fabrication up to a height of 5 mm (Yang et al. 2015). Fluorescently labeled human chondrocytes and osteogenic progenitors suspended in alginate have also been used for constructing 3D grafts (Fedorovich et al. 2011). p (HPMAm-lac)-PEG-p (HPMAm-lac)-based hydrogel fibers were generated that showed thermosensitivity as well as photopolymerizability; 3D cell-laden scaffolds were prepared, which demonstrated good mechanical properties and tunable degradation (Censi et al. 2011). Beside the aforementioned methods, use of other techniques such as SLS has been reported. In addition, combinatorial methods have been investigated using materials such as PCL (Chen et al. 2014a) as the fabrication substrate in SLS and modification with polymers such as gelatin (Chen et al. 2011) and collagen (Chen et al. 2014b). Table 2 lists the various additive manufacturing techniques used to generate scaffolds for cartilage regeneration highlighting studies that have investigated bioprinting applications.

4 Muscle

In studies related to skeletal muscle regeneration, structures are mostly bioprinted. Structures have remained essentially two dimensional (in the form of cell sheets) rather than solid volumetric scaffolds. The two primary uses of additive manufacturing in the case of skeletal muscle have been to generate aligned cell growth for improved tissue morphogenesis and to obtain spatial control of growth factors for supporting directed tissue growth. Scaffolds made of directional parallel fibers stimulate muscle cells to grow in an aligned manner and support further myoblast growth, fusion, and myotube formation (Liang et al. 2007; Wang et al. 2012; Ostrovidov et al. 2014). Various approaches have been developed to support the fabrication of aligned fibers, including electrospinning (San Choi et al. 2008) and wet spinning (Razal et al. 2009). AM technologies such as ink-jet bioprinting (Seol et al. 2014) have also been employed to pattern various growth factors on material surfaces (Jose et al. 2016). This approach has been used to pattern fibroblast growth factor-2 (Campbell et al.

Table 2 Various AM techniques used in cartilage tissue regeneration

Category	Method	Publication	Cell density (cell/ml)	Porosity	Cell viability	Modulus (KPA)	Material	Cell type	Bioprinting
Binder jetting	Ink-jet printing	(Cui et al. 2012b)	–	–	89	395.73 – 80.40	PEGDMA	Human articular chondrocytes	Yes
		(Cui et al. 2014)	5×10^6	–	90	–	PEGDA	Chondrocyte	Yes
		(Gao et al. 2015b)	6×10^6		87.9 ± 5.3%	33–67	Acrylated poly (ethylene glycol) (PEG)	Human mesenchymal stem cells (hMSCs)	Yes
		(Cui et al. 2012c)	8×10^6 and 20×10^6	–	84.9 ± 2.2%	36.90 ± 3.41 and 29.88 ± 2.33	PEGDMA	Human articular chondrocyte	Yes
		(Xu et al. 2012)	$3–4 \times 10^6$	–	81.58 ± 3.46%	0.41–1.76	PCL-collagen	Articular chondrocytes	Yes
	Powder bed and ink-jet 3D printing (PBIH)	(Sherwood et al. 2002)	–	25–55	–	Tensile, 83–233; compressive, 54–450 Mpa	d,l-PLGA/l-PLA and l-PLGA/TCP	Chondrocytes	No
Vat photopolymerization	SLA	(Schüller-Ravoo et al. 2013)	–	54.0 ± 2.2%	–	100	Poly (trimethylene carbonate)	Bovine chondrocytes	No
		(Melchels et al. 2009)	–	73	–	56 ± 2 Mpa	PDLLA	Mouse pre-osteoblasts (MC3T3 cell line)	No
		(Elomaa et al. 2011)	–	70.5 ± 0.8%	–	6.7–15.4 Mpa	PCL	NIH3T3 fibroblasts	No
		(Sun et al. 2015)	4×10^6	–	84	780	Poly-d,l-lactic acid/ polyethylene glycol/ poly-d,l-lactic acid (PDLLA-PEG)/ hyaluronic acid (HA)	Human adipose-derived stem cell	Yes

(*continued*)

Table 2 (continued)

Category	Method	Publication	Cell density (cell/ml)	Porosity	Cell viability	Modulus (KPA)	Material	Cell type	Bioprinting
		(Linzhong et al. 2010)	–	–	–	4.54 MPa	Acrylamide	–	No
	Two-photon printing	(Weiß et al. 2009)	–	–	–	–	?	Bovine chondrocytes	No
		(Weiß et al. 2011)	–	–	–	–	Poly (ethylene glycol diacrylate) (PEGDA) and acrylamide	Bovine chondrocytes	No
	uSLA	(Lee et al. 2007a)	–	–	–	8.72–519.1 Mpa	PPF/DEF	Fibroblast	No
		(Lee et al. 2008)	–		–		TMC/TMP	–	No
Material extrusion	Fused deposition modeling (FDM)	(Cao et al. 2003)	–	–	–	–	PCL	Chondrocytes	No
		(Hsu et al. 2007)	–	52–97	–	–	PLA-PCL	Chondrocytes	No
		(Woodfield et al. 2004)	–	55–87	–	0.05–2.5	Poly (ethylene glycol)-terephthalate-poly (butylene terephthalate) (PEGT/PBT)	–	No
		(Yen et al. 2009)	–	47–97	–	Storage moduli: 2.5–8 MPa	PLGA collagen	Chondrocytes	No

	Liquid-frozen deposition	(Yen et al. 2008)	–	45–78	–	Storage modulus: 0.26–5.68 MPa	PLGA	Chondrocytes	No
		(Hsu et al. 2011)	–	49.46–5.48%	–	–	PLGA/alginate	Human placenta-derived mesenchymal stem cells (hPMSCs)	Yes
		(Hung et al. 2014)	–	–	–	1.66 ± 0.06 MPa	Polyurethane (PU)-polyethylene oxide (PEO)- polylactic-co-glycolic acid (PLGA)	Chondrocytes	No
	Material extrusion	(Moroni et al. 2006)	–	–	–	–	Poly (ethylene oxide-terephthalate)-co-poly (butylene terephtalate) (PEOT/PBT)	Chondrocytes	No
		(Fedorovich et al. 2011)	MSCs and Chs: $5 \cdot 106$ and $3 \cdot 10^6$ cells/mL	89	35–66	4.5–7.6	Alginate	Human chondrocytes	Yes
		(Censi et al. 2011)	5.0×10^6	–	94 ± 3	119	Poly (N-(2-hydroxypropyl) methacrylamide lactate) A-block	Chondrocyte	Yes
Powder bed fusion	SLS	(Chen et al. 2014a)	–	74–77	–	–	PCL	Chondrocyte	No
		(Chen et al. 2011)	–	76.2	–	7.22 ± 0.18 MPa	Gelatin-PCL	Chondrocyte	No
		(Chen et al. 2014b)	–	70–82	–	2–3.8 MPa	PCL-collagen	Chondrocytes	No

2005) or bone morphogenetic protein-2 onto submicrometer polystyrene fibers (Ker et al. 2011). In another study, the same method has been reported for growth factor patterning, which enabled spatial control of stem cell fate on fibrin films (Phillippi et al. 2008). Mesenchymal stem cells are sensitive to the topography of the scaffolds (Patz et al. 2005); it should be noted that the aforementioned designs are limited to two-dimensional structures. 3D scaffolds have been developed by combining electrospinning methods with other techniques to make 3D structures such as nanofiber yarn/hydrogel core-shell scaffolds (Wang et al. 2015). Other techniques, including UV-embossed microchannels, have shown the potential for highly structured skeletal muscle tissue morphogenesis (Ramón-Azcón et al. 2013).

Extrusion-based manufacturing is the most commonly used method for muscle scaffold fabrication. Synthetic polymers such as PCL and PEO have been modified with natural polymers such as alginate for use in muscle regeneration. Scaffold fabrication is performed by extrusion to form a sheet, which is then rolled into a 3D tube to prepare volumetric constructs containing evenly distributed C2C12 cells (Yeo et al. 2016). In vivo results indicate that the myoblasts proliferate within the constructs and that myosin heavy chain (MHC, a marker of myogenic differentiation) expression were influenced by the alignment of extruded fibers (Yeo et al. 2016). Alginate and gelatin have also been printed on 3D scaffolds for muscle regeneration using extrusion-based techniques. These studies demonstrated that the ink formulation was a major factor that determined the mechanical properties, fluid transport, and cell viability for the constructs. The extrusion pressure associated with scaffold synthesis did not have a significant influence on myoblast viability within the investigated range (between 4 and 9.5 psi) (Chung et al. 2013b).

Skeletal muscle regeneration in volumetric defects requires mechanical properties comparable to native tissue, high cell density, and high viability for transplantation. The local cell density affects myoblast fusion and fiber formation; the transport properties of the scaffold are essential for maintenance of tissue viability while vascular infiltration occurs. In an attempt to focus on improving cell seeding efficiency, alginate and cells have been used as a bioink in scaffolds that were reinforced with PCL fibers (Yeo et al. 2016). It was observed that PCL/alginate scaffolds laden with cells within alginate fibers showed the highest cell density homogeneity and better cellular behavior; other samples, including cell-coated PCL/alginate scaffolds and cell-free PCL/alginate scaffolds, exhibited better mechanical properties (Yeo et al. 2016). Co-deposition of fibers remains a crucial strategy in 3D scaffold manufacturing (Malda et al. 2013); synthetic polymers such as PCL provide the mechanical backbone within constructs and hydrogels such as alginate serve as "sacrificial" temporary carriers for cells, growth factors, and biologics. This strategy allows for independently tuning the microenvironment and mechanical properties for optimal cell density and viability. Additionally, extrusion-based methods have been used in fused deposition modeling to fabricate PCL and composite hydrogels made of gelatin, fibrinogen, hyaluronic acid, and glycerol (Kang et al. 2016). Gelatin exhibits a thermosensitive response in gels below 25 °C, while fibrinogen has been used to provide matrix stability for enhancing

cell growth (Kang et al. 2016). Hyaluronic acid and glycerol were introduced as dispenser agents to prevent nozzle clogging. In vivo results show that cell-laden scaffolds have the potential to be directly used for production (Kang et al. 2016) of the skeletal muscle. A variant of this approach has the potential to be used for restoration of bone and cartilage defects. Figure 5 shows data from the bioprinted muscle (Kang et al. 2016).

Additive manufacturing lends itself well to recreating the challenging transition at various orthopedic interfaces, where multiple orders of magnitude of mechanical properties are traversed within small length scales. Integrated tendon-muscle units have been previously fabricated using multichannel nozzles. The material used was a thermoplastic polyurethane, which was co-printed with a bioink containing muscle cells. The muscle component was transitioned to a tendon site graft, which was fabricated using PCL and NIH/3 T3 cell hydrogel-based bioink. The bioink contained hyaluronic acid in addition to gelatin and fibrinogen (Merceron et al. 2015). Results show that the printed complex structure simulates vastly different mechanical properties on the muscle and tendon sides while achieving homogenous cell distribution and maintaining good cell viability (Merceron et al. 2015). AM has great promise for muscle graft fabrication; however, it has not been evaluated as much as additive manufactured bone and cartilage grafts due to the need for high cell density over large volumes and the need for pre-vascularization. A summary of the current state of the art in skeletal muscle bioprinting is shown in Table 3.

5 Tendons and Ligaments

Tendon reconstruction with biologically active scaffolds is hampered by many issues, including the restoration of a highly organized matrix architecture, low cellularity, the need for high cell viability, zones of differential mechanical properties within the matrix, a transition from a stiff tissue to a soft tissue at the interfaces, and a functional need for force transmission. Simulating the collagen fibril orientation and organization to match native tendon tissue has been the most challenging requirement. Different techniques, such as electrospinning (Verdiyeva et al. 2015), wet spinning (Kew et al. 2012), and melt spinning (Webb et al. 2013), have been utilized to produce micro- or nanofibers that resemble the native tissue (Regeneration 2015). Natural polymers such as silk (Sahoo et al. 2010; Shen et al. 2012; Qiu et al. 2013) and collagen type I have been used in tendon tissue regeneration (Kew et al. 2012; Oryan et al. 2013; Xu et al. 2013b); however, the lack of fiber formation and poor mechanical properties have been the drawbacks associated with the use of these materials. Synthetic polymers such as PLLA (Barber et al. 2011), PCL (Kazimoğlu et al. 2003), polydioxanone (Oryan et al. 2013), PLA (Sato et al. 2000), PGA (Chen et al. 2012), and PLGA (Sahoo et al. 2010) have also been used to generate organized fiber scaffolds; among these materials, PLGA is the most commonly used material (Ouyang et al. 2003; Sahoo et al. 2006).

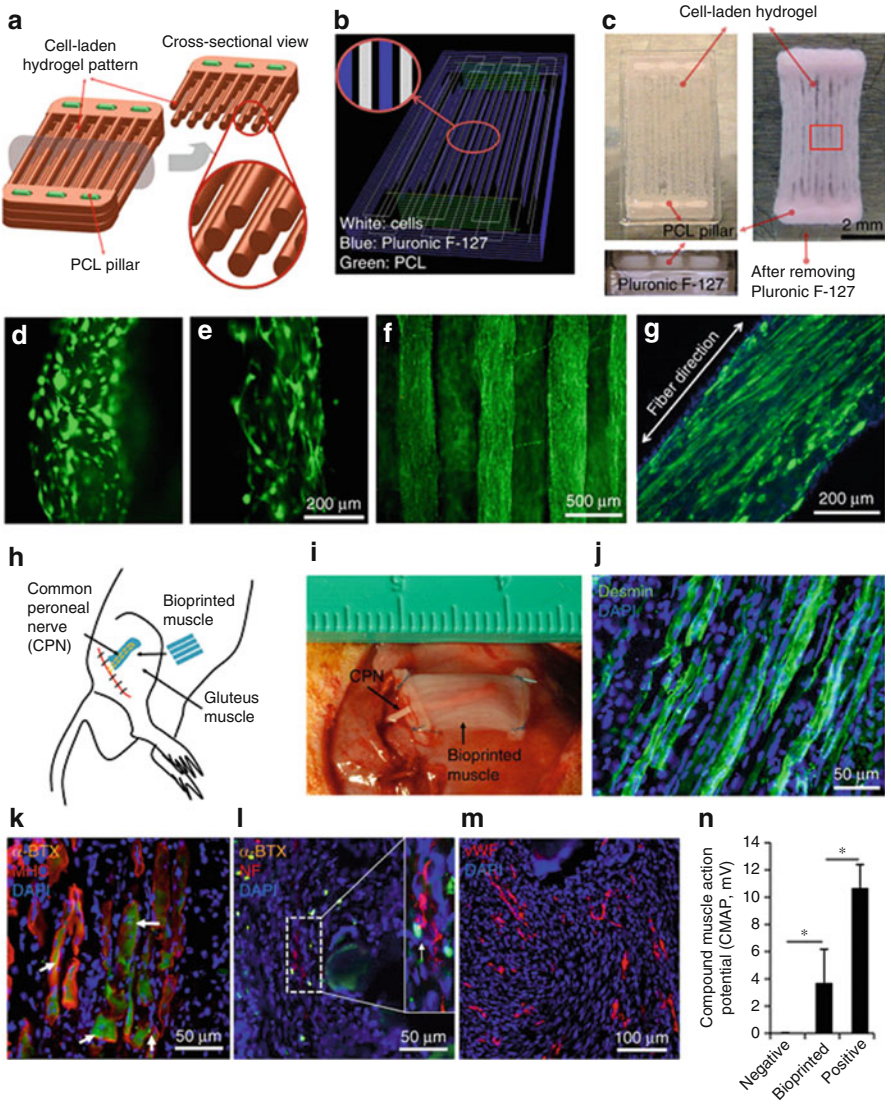

Fig. 5 In vitro bioprinted muscle. (**a**) Designed fiber bundle structure for muscle organization. (**b**) Visualized motion program for 3D printing muscle construct. Lines of green, white, and blue indicate the dispensing paths of PCL, cell-laden hydrogel and sacrificial material, respectively. (**c**) 3D patterning outcome of designed muscle organization (left) before and (after) removing the sacrificial material (Pluronic F127). (**d**, **e**) The PCL pillar structure is essential to stabilize the 3D-printed muscle organization and to induce a compaction phenomenon of the patterns of the cell-laden hydrogel that causes cell alignment in a longitudinal direction of the printed constructs, without PCL pillar (**d**) and with PCL pillar (**e**). The cells with PCL pillar showed unidirectionally organized cellular morphologies that are consistently aligned along the longitudinal axis of the printed construct, which is in contrast to the randomly oriented cellular morphologies without PCL

Additive manufacturing has been leveraged to simulate fibers with appropriate tensile properties similar to those of the tendon and ligaments (Kim et al. 2016). Among available AM technologies, Bioplotters, in particular, have been utilized for tendon scaffold fabrication (Chung et al. 2013a). This method is based on the extrusion of bioink through different channels to deposit cells and other materials to form a 3D structure. One example is of cells suspended in hyaluronic acid and later printed in a collagen solution using a Bioplotter. Authors suggest that this approach is applicable to other scaffolds as a self-assembling coating. For example, PLLA scaffolds prepared using a Bioplotter have been coated with the collagen-hyaluronic acid membrane. The results demonstrated improvement of implant bioactivity, indicating that this coating may serve as a tissue binder (Chung et al. 2013a).

In another study, a custom-developed electrodynamic jet printing system has been used to fabricate a PCL mat (Wu et al. 2015). The printed mat was made of two types of fibers with different thicknesses and then rolled to form a 3D structure. Mechanical testing indicated that an increase in fiber diameter (20–75 μm) led to improved mechanical properties. Moreover, the design exhibited the ability to support the attachment and growth of human tenocytes. Cell alignment and morphology indicated the formation of a tendon-like architecture and upregulation of collagen type I expression, indicating the suitability of the construct for tendon restoration.

Ligament injuries are the other crucial concerns in orthopedic health care. AM offers a different approach to develop new treatments for ligament injuries, which are more focused on improving the transitions at bone-ligament interfaces; these interfaces are often observed to be the sites of failures in synthetic graft restorations. In addition to the tensile and other mechanical properties of the graft, properties such as osteogenicity matter as well. In one approach, customized cages for anterior cruciate ligament (ACL) treatments were developed using AM technologies. A low-temperature 3D printing method was used to manufacture ligament implants from TCP for cranial cruciate ligament treatment (Castilho et al. 2014). In this study, TCP powder was sintered before printing; the milled powder was later mixed with phosphoric acid. The graft was air-dried at room temperature, and the residual powders were removed. The in vivo results indicated that an optimized cage performance resulted in mechanical properties similar to those of the trabecular bone and that limb function was restored without any complication (Castilho et al. 2014). Treatment of cruciate ligament rupture through 3D-printed biodegradable cages was optimized computationally for survival in a preclinical canine model.

Fig. 5 (continued) pillar. (**f**) The live/dead staining of the encapsulated cells in the fiber structure indicates high cell viability after the printing process (green, live cells; red, dead cells). (**g**) Immunofluorescent staining for myosin heavy chain of the 3D-printed muscle organization after 7-day differentiation. (**h**–**m**) Structural maintenance and host nerve integration of the bioprinted muscle construct in in vivo study. (**h**) Schematic diagram of ectopic implantation of bioprinted muscle construct in vivo. (**i**–**k**) The bioprinted muscle construct was subcutaneously implanted with the dissected common peroneal nerve. (Kang et al. 2016)

Table 3 Studies reported the synthesis of muscle scaffolds based on different AM techniques

Category	Method	Publication	Material	Cell type	Cell density (cell/ml)	Porosity %	Cell viability%	Modulus (KPA)	Bioprinting
Material extrusion	Material extrusion	(Yeo et al. 2016)	PCL-alginate-PEO	C2C12 myoblast cells	1×10^7	–	95.2 ± 2.8	43–48	Yes
		(Ahn et al. 2012)	Alginate	(MC3T3-E1)	$(1.7–2.3) \times 10^6$	–	84	–	Yes
		(Chung et al. 2013b)	Alginate	BL6 primary myoblast	5×10^5	–	92–98	1.5–12	Yes
		(Lee et al. 2013)	PCL-alginate	MC3T3-E1	1×10^5	62–68	62–83	4.1–5.1 MPa	Yes
		Kang (Kang et al. 2016)	PCL-gelatin-fibrinogen-ha-glycerol	C2C12 myoblast cells	5×10^6	70	95	–	Yes
		(Merceron et al. 2015)	PCL-gelatin-fibrinogen-ha-glycerol	NIH/3 T3	40×10^6	–	c2c12, 94; NIH/3 T3, 83	Muscle side, 0.39 ± 0.05 Mpa; tendon side, 46.67 ± 2.67 Mpa; interface region, 1.03 ± 0.14 Mpa	Yes

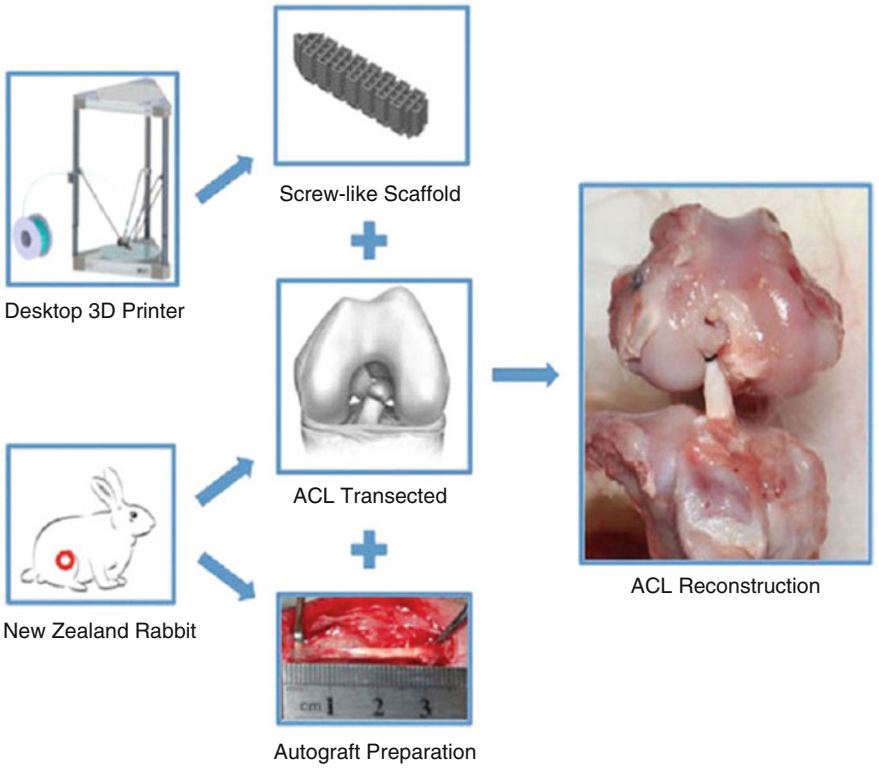

Fig. 6 Porous PLA screwlike scaffold with hydroxyapatite coating as a ligament surgical implant. (Liu et al. 2016)

A low-temperature 3D printing method was developed to synthesize TCP scaffolds with varying porosity in an attempt to optimize mechanical properties that maximized both the porosity to promote bone infiltration and the strength to survive in physiological environments. It was found that the printing direction affected the porosity and overall structural properties (Castilho et al. 2013).

ACL reconstruction has also been performed using a 3D-printed PLA screwlike implant (Liu et al. 2016). The scaffold has been evaluated in a rabbit model using a PLA scaffold that was coated with hyaluronic acid in order to improve its osteoconductivity. Both in vitro and in vivo studies were conducted to evaluate cell proliferation, osteogenicity, and bone regeneration on the graft surface. This 3D printing technology was based on FDM; PLA was extruded into the porous scaffold through a heated nozzle. The results of this study demonstrated that the seeded scaffolds had improved in vivo outcomes compared to cell-free scaffolds; in addition, they offered the ability of "fabricating surgical implants at the clinic" (fab@clinic) as a cost-effective and practical technique (Liu et al. 2016). Figure 6 shows a 3D-printed anterior cruciate ligament surgical implant (Liu et al. 2016). Table 4 shows the studies conducted on ligament regeneration using various AM techniques.

Table 4 Studies reported the synthesis of ligaments and tendon scaffolds based on different AM techniques

Category	Method	Publication	Material	Cell type	Porosity	Pore size (μM)	Elastic modulus (MPa)	Bioprinting
Binder jetting	Powder bed and ink-jet 3D printing (PBIH)	(Castilho et al. 2014)	TCP-DCP	In vivo	59	1000	7.27–19.8	No
Material extrusion	Fused deposition modeling (FDM)	(Liu et al. 2016)	PLA/HA	In vivo	42 ± 5	220	–	No
	Low-temperature deposition manufacturing (LDM)	(Castilho et al. 2013)	TCP	–	38–41	500–1000	–	–

6 Cardiovascular System

Bioprinters are used in various cardiovascular research applications (Moldovan et al. 2017). Cardiovascular diseases are the leading causes of death worldwide (Mosadegh et al. 2015); perhaps the most critical long-term goal in cardiovascular research is to create a human heart for transplantation. As the population is aging, the number of patients requiring organ replacement is increasing (Atala 2009). In addition, the number of new cases of organ failure is growing. On the other hand, the number of organ donors is not sufficient to accommodate patients on waiting lists for organ transplantation, thus creating an organ shortage crisis (Shafiee and Atala 2017). The second important challenge in cardiovascular system research (and in tissue engineering in general) is to manufacture vascularized tissue (Forgacs 2012). Creating thick tissues requires their vascularization, which is indispensable for providing nutrition and removing waste from cells located in tissues thicker than 200 μm (Shafiee and Atala 2017). Large vascular grafts are also required for patients with certain diseases (Pashneh-Tala et al. 2016). Engineering tubular biological structures with particular cell types (including endothelial, smooth muscle, and fibroblast cell types) with properties that are appropriate for creating blood vessels such as suture retention strength and burst pressure resistance is essential. Another unmet need for patients with cardiovascular disease is cardiac patches that replace damaged tissues of an infarcted heart (Weinberger et al. 2017). The engineered heart valve is also a remedy for patients with diseases like pulmonary valve stenosis and bicuspid aortic valve disease (Cheung et al. 2015). The engineering and fabrication of such complex biological structures require advanced technologies and techniques. Bioprinters, with their unique capabilities to create complex tissue structure precisely, automatically, and reproducibly hold promise to advance cardiovascular research (Shafiee and Atala 2016).

In tissue engineering, organs are categorized into four different levels of complexity (Shafiee and Atala 2017). Flat tissues and organs such as the skin are the least complex level. The clinical feasibility of engineering flat tissue fabrication has previously been shown (Centanni et al. 2011). Tubular organ structures such as the tracheas are the next level of complexity, followed by hollow non-tubular organ structures. The latter structures, which include organs such as the bladder, have been engineered in vitro and successfully transplanted into the patients (Atala et al. 2006). However, the most complex organs to fabricate are solid organs such as the liver, kidney, and heart. Therefore, bioprinting the heart with current state-of-the-art technology remains a challenge.

Tissue vascularization is another challenge in the field of tissue engineering in general and cardiovascular research in particular. Bioprinting has been used extensively as an effective biofabrication technique for vascularization. In one study, bioprinters were used to print a mixture of sucrose/glucose/dextran as a self-supporting and interconnected lattice (Miller et al. 2012). The lattice was then used as the sacrificial component of a 3D vascular design. The network of adjacent living cells provided appropriate mechanical stiffness and biocompatibility. The

lattice was encapsulated in the ECM; the lattice was then dissolved in a culture medium to leave its imprint. The lattice imprint was subsequently perfused with endothelial cells to be used as the capillary network throughout the tissue. In another study, 3D biomimetic microvascular networks were printed using an omnidirectional printing system (Wu et al. 2011). The network was printed in a hydrogel matrix using a fugitive organic ink patterned in a thermal or photocurable gel reservoir. After photopolymerization of the gel, the fugitive ink was removed under a modest vacuum, leaving a uniform microchannel interconnected network. The technique is able to create complex vascular networks by printing inside the gel reservoir. In another seminal work, 1 cm-thick 3D cell-laden, vascularized tissues were printed (Kolesky et al. 2014; Kolesky et al. 2016). The printed tissues were perfused on a chip for more than 6 weeks; the thickness and the durability accomplished in this method were the highest record achieved in the field to date. A fugitive ink was made of Pluronic F127, thrombin, and transglutaminase, which was used to make the imprint of empty channels as the vascular network. The structure was made by integration of the parenchyma, stroma, and endothelium using bioinks of human mesenchymal stem cells (hMSCs) and human neonatal dermal fibroblast cells. The ECM was customized with embedded vasculature, which was lined with human umbilical vein endothelial cells (HUVECs). The 3D vascularized tissues were perfused with growth factors and demonstrated differentiation of the hMSCs to an osteogenic lineage in situ.

Fabrication of blood vessels using various biofabrication techniques, particularly bioprinting, has been a recent focus of attention. Spherical and cylindrical bioink particles composed of different cell types (e.g., human umbilical vein smooth muscle cells and human skin fibroblasts) were printed using extrusion printers; agarose rods were used as support (Norotte et al. 2009) (Fig. 7a–d). Tubular 3D structures underwent self-assembly, and the bioink particles fused to each other (Fig. 7e and f). The fusion of these discrete multicellular systems rendered the structure physically strong, facilitating its transfer to the bioreactor and subsequent maturation. Each cell type relocated to the physiologically appropriate location in the structure through another self-assembly procedure called cell sorting. Predictive modeling to study the shape evolution of multicellular systems was used to predict the fusion time and transfer of the 3D-printed tissue to the bioreactor at the optimal time (when the fusion was complete) (McCune et al. 2014) (Fig. 7g and h). The model successfully predicted the characteristic fusion time for cellular bioink particles with different geometries such as spherical and cylindrical cellular inks (Shafiee et al. 2015). Finally, a biophysical parameter of the bioink particles was introduced to accelerate the tissue maturation process (Shafiee et al. 2017). It was shown that the apparent tissue surface tension (ATST), a viscoelastic characteristic of cellular bioinks, was tunable by various preparation techniques. More importantly, it was demonstrated that cellular bioinks with higher ATST values fused faster than cellular bioinks comprising the same cell types but with lower ATST values. This acceleration translated to a higher adhesion strength of cells on those cellular bioinks with higher surface tension values. The effect of ATST on faster fusion may eventually accelerate the tissue maturation time post-bioprinting.

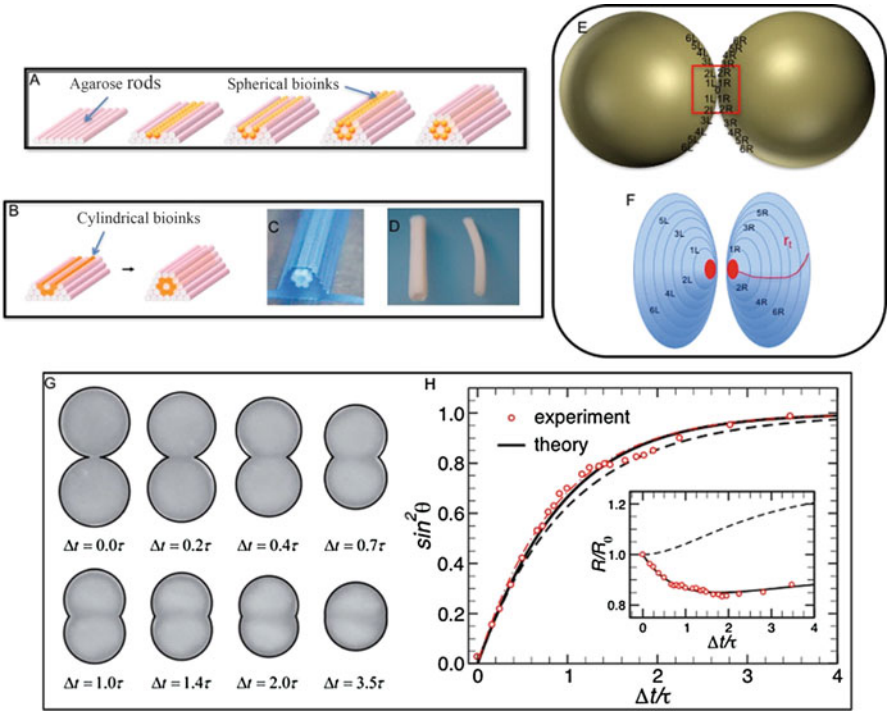

Fig. 7 (**a**) Bioprinting of tubular organ structures using spherical cellular bioinks. Agarose rods were used as support to build 3D structures. (**b**) Cylindrical cellular bioink was also used to make tubular bioprinted structures. (**c**) Bioprinted blood vessels right after the printing procedure. (**d**) The biological structures after fusion of cellular bioink particles. (**a**–**d** are adapted from Norotte et al. 2009 with permission from Elsevier). (**e**) Schematic demonstration of fusion of two spherical cellular bioinks. To commence the fusion, the aggregates are placed close to each other. The fusion starts by the development of bonds among adhesion molecules of first initial cells from each aggregate. (**f**) The fusion process continues by attachment of imaginary strips of cells (1, 2, 3,. . ., n) from the right (R) and left (L) aggregate. (**e** and **f** are adapted from Shafiee et al. 2017 with permission from Elsevier). (**g**) Snapshots of two fusing cellular bioink particles (initial radius 274 μm) made out of human skin fibroblast (HSF) cells. Over the period of fusion, two aggregates evolve to a single one while the volume decreases. (**h**) The fusion process can be predicted quantitatively. The red circles are showing the experimental results of fusing HSF aggregates. Theoretical Ashkan with consideration of a change in volume (solid curve). The dashed curve represents the theoretical fit without consideration of the change in volume. Inset: shows the change in radius of the aggregates. (**g** and **h** are adapted from McCune et al. 2014 with permission from the Royal Society of Chemistry)

Myocardial infarction causes serious damage to the heart muscle and is associated with a high mortality rate. The heart has limited capability for tissue regeneration and repair (Chiong et al. 2011). It has been shown that transplantation of cardiac patches may significantly enhance functional recovery (Gaebel et al. 2011). Bioprinted cardiac patches have been tested in vitro and in vivo with promising outcomes (Gao et al. 2017). In one study, hMSCs and HUVECs were printed on polyester

urethane urea. These cells were patterned using laser bioprinters; the patches were used for cardiac regeneration in rats with induced myocardial infarctions. This resulted in vessel formation, enhancement of angiogenesis, and eventually improved heart function. Using multiphoton-excited 3D printing, native-like ECM scaffolds were generated. The system created a scaffold with submicrometer resolution, which was seeded with human-induced pluripotent stem cell-derived cardiomyocytes, smooth muscle, and endothelial cells. The generated human-induced pluripotent stem cell-derived cardiac muscle patches (hCMPs) were then evaluated in a murine model. The hCMPs, which were generated with bioprinted ECM-based scaffolds, showed significantly improved recovery from ischemic myocardial injury. High levels of cell engraftment and enhancement of cardiac function were observed. In another study, bioink particles prepared with decellularized ECM were used to print cell-laden constructs of heart tissues (Pati et al. 2013). These bioinks can provide an appropriate microenvironment for the cells similar to that of natural ECM. The printed structures showed stability and produced essential cues for proliferation and engraftment.

Patients may need replacement of their heart valves. The current options are either biological heart valve prostheses or mechanical prostheses (Bloomfield 2002). For biological heart valve prostheses, autologous samples are the most desirable. However, the complex heterogeneous structure of the heart valve makes it difficult to fabricate prostheses from autologous tissue. As such, 3D-printing technologies are being used to create biological heart valve prostheses for patients.

In a series of studies, appropriate heart valve geometries with root walls and tri-leaflets were created using 3D printing. Anatomical heterogeneous valve conduits were fabricated by 3D hydrogel printing with controlled photocrosslinking (Hockaday et al. 2012); polyethylene glycol-diacrylate hydrogels in addition to alginate were used in this study. The scaffolds were seeded with porcine aortic valve interstitial cells and were cultured for 21 days; over this time, the cells maintained viability. Aortic root sinus smooth muscle cells and aortic valve leaflet interstitial cells were encapsulated in alginate/gelatin hydrogel to bioprint valve conduits. The structures showed viability over 7 days in culture (Duan et al. 2013). The production of anatomically accurate living valve scaffolds using bioprinting demonstrated the unique possibilities of bioprinting in valve prosthesis fabrication (Duan et al. 2014). Valvular interstitial cells were encapsulated in hybrid hydrogels composed of methacrylated hyaluronic acid and methacrylated gelatin. The encapsulated cells maintained high viability (>90%) in depths exceeding 700 μm below the surface. The hybrid hydrogel composition could regulate the cellular response and support encapsulated cells.

7 Conclusions

Unique capabilities of bottom-up processes, such as additive manufacturing, include the ability to spatially pattern cells within materials. Significant research efforts have been undertaken to accomplish different architectures and designs of additive

manufacturing-produced scaffolds. Currently unachievable scaffold designs with transitions at tissue interfaces (e.g., bone-ligament or muscle-tendon or bone-cartilage interfaces) or constructs with integrated tissue regions (e.g., blood vessels within the bone or nerves and blood vessels within the skeletal muscle) can be tackled with appropriate advances in bioprinting. Moreover, the application of bioprinters in cardiovascular research has brought much hope to patients in need of heart valves or cardiac patches. Moreover, by fabricating vascularized tissues, the tissue engineering field has benefited immensely from bioprinting technology. However, more sophisticated applications and whole human organ fabrication are still far from coming to fruition using current technology. Therefore, fabrication of solid organs such as the heart, liver, and kidney using bioprinters remains a long-term challenge to overcome. Current challenges in the field include the maintenance of cell viability and graft patency not only during the process of deposition but over the duration of the volumetric print. The translation of these grafts from the benchtop to preclinical animal models is essential to begin envisaging future clinical trials for restorative human surgery. Advances in 3D printing and bioprinting technology have outpaced the available bioinks and scaffold morphologies as well as the specific understanding of precise cell density and distribution required for graft success. While additive manufacturing already offers significant advantages in the manufacture of custom metallic and ceramic implants for orthopedic stabilization, the amalgamation of cellular and material research in bioprinting promises to offer advanced biosynthetic grafts for regeneration and restoration of tissue deficits instead of mere stabilization.

References

Ahmadi S et al (2014) Mechanical behavior of regular open-cell porous biomaterials made of diamond lattice unit cells. J Mech Behav Biomed Mater 34:106–115

Ahn S et al (2012) Cells (MC3T3-E1)-laden alginate scaffolds fabricated by a modified solid-freeform fabrication process supplemented with an aerosol spraying. Biomacromolecules 13(9): 2997–3003

Ahn S et al (2013) Functional cell-laden alginate scaffolds consisting of core/shell struts for tissue regeneration. Carbohydr Polym 98(1):936–942

Atala A (2009) Engineering organs. Curr Opin Biotechnol 20:575–592

Atala A, Yoo JJ (2015) Essentials of 3D biofabrication and translation. Academic Press, Cambridge, MA

Atala A, Bauer B, Soker S, Yoo J, Retik A (2006) Tissue-engineering autologous bladders for patients needing cystoplasty. Lancet 367:1241–1246

Aviss K et al (2010) Aligned electrospun polymer fibres for skeletal muscle regeneration. Eur Cell Mater 19:193–204

Barber JG et al (2011) Braided nanofibrous scaffold for tendon and ligament tissue engineering. Tissue Eng A 19(11-12):1265–1274

Barry JJ et al (2008) In vitro study of hydroxyapatite-based photocurable polymer composites prepared by laser stereolithography and supercritical fluid extraction. Acta Biomater 4(6): 1603–1610

Barucca G et al (2015) Structural characterization of biomedical co–Cr–Mo components produced by direct metal laser sintering. Mater Sci Eng C 48:263–269

Bertol LS et al (2010) Medical design: direct metal laser sintering of Ti–6Al–4V. Mater Des 31(8): 3982–3988
Bhumiratana S, Vunjak-Novakovic G (2012) Concise review: personalized human bone grafts for reconstructing head and face. Stem Cells Transl Med 1(1):64–69
Bian W et al (2011) Design and fabrication of a novel porous implant with pre-set channels based on ceramic stereolithography for vascular implantation. Biofabrication 3(3):034103
Biemond J et al (2013) Bone ingrowth potential of electron beam and selective laser melting produced trabecular-like implant surfaces with and without a biomimetic coating. J Mater Sci Mater Med 24(3):745–753
Bloomfield P (2002) Choice of heart valve prosthesis. Heart 87:583–589
Bobbert F et al (2017) Additively manufactured metallic porous biomaterials based on minimal surfaces: a unique combination of topological, mechanical, and mass transport properties. Acta Biomater 53:572–584
Boland T et al (2006) Application of inkjet printing to tissue engineering. Biotechnol J 1(9): 910–917
Bose S et al (2003) Pore size and pore volume effects on alumina and TCP ceramic scaffolds. Mater Sci Eng C 23(4):479–486
Bose S et al (2013) Bone tissue engineering using 3D printing. Mater Today 16(12):496–504
Bsat S et al (2015) Effect of alkali-acid-heat chemical surface treatment on electron beam melted porous titanium and its apatite forming ability. Materials 8(4):1612–1625
Campbell PG et al (2005) Engineered spatial patterns of FGF-2 immobilized on fibrin direct cell organization. Biomaterials 26(33):6762–6770
Campoli G et al (2013) Mechanical properties of open-cell metallic biomaterials manufactured using additive manufacturing. Mater Des 49:957–965
Cao T et al (2003) Scaffold design and in vitro study of osteochondral coculture in a three-dimensional porous polycaprolactone scaffold fabricated by fused deposition modeling. Tissue Eng 9(4, supplement 1):103–112
Carignan RG, et al (1990) Thumb joint prosthesis, Google Patents
Castilho M et al (2013) Fabrication of computationally designed scaffolds by low temperature 3D printing. Biofabrication 5(3):035012
Castilho M et al (2014) Application of a 3D printed customized implant for canine cruciate ligament treatment by tibial tuberosity advancement. Biofabrication 6(2):025005
Censi R et al (2011) A printable Photopolymerizable thermosensitive p (HPMAm-lactate)-PEG hydrogel for tissue engineering. Adv Funct Mater 21(10):1833–1842
Centanni J, Straseski J, Wicks A, Hank J, Rasmussen C, Lokota M, Schurr M, Foster K, Faucher L, Caruso D, Comer A, Allen-Hoffmann B (2011) StrataGraft skin substitute is well-tolerated and is not acutely immunogenic in patients with traumatic wounds: results from a prospective, randomized, controlled dose escalation trial. Ann Surg 253(4):672–683
Chen C-H et al (2011) Effects of gelatin modification on rapid prototyping PCL scaffolds for cartilage engineering. J Mech Med Biol 11(05):993–1002
Chen B et al (2012) In vivo tendon engineering with skeletal muscle derived cells in a mouse model. Biomaterials 33(26):6086–6097
Chen C-H et al (2014a) Surface modification of polycaprolactone scaffolds fabricated via selective laser sintering for cartilage tissue engineering. Mater Sci Eng C 40:389–397
Chen C-H et al (2014b) Selective laser sintered poly-ε-caprolactone scaffold hybridized with collagen hydrogel for cartilage tissue engineering. Biofabrication 6(1):015004
Cheng X et al (2012) Compression deformation behavior of Ti–6Al–4V alloy with cellular structures fabricated by electron beam melting. J Mech Behav Biomed Mater 16:153–162
Cheung D, Duan B, Butcher J (2015) Current progress in tissue engineering of heart valves: multiscale problems, multiscale solutions. Expert Opin Biol Ther 15(8):1155–1172
Chiong M, Wang Z, Pedrozo Z, Cao D, Troncoso R, Ibacache M, Criollo A, Nemchenko A, Hill J, Lavandero S (2011) Cardiomyocyte death: mechanisms and translational implications. Cell Death Disease 2:e244

Choi J-W et al (2009) Fabrication of 3D biocompatible/biodegradable micro-scaffolds using dynamic mask projection microstereolithography. J Mater Process Technol 209(15):5494–5503
Chung EJ et al (2013a) In situ forming collagen–hyaluronic acid membrane structures: mechanism of self-assembly and applications in regenerative medicine. Acta Biomater 9(2):5153–5161
Chung JH et al (2013b) Bio-ink properties and printability for extrusion printing living cells. Biomater Sci 1(7):763–773
Ciocca L et al (2011) Direct metal laser sintering (DMLS) of a customized titanium mesh for prosthetically guided bone regeneration of atrophic maxillary arches. Med Biol Eng Comput 49 (11):1347–1352
Claeyssens F et al (2009) Three-dimensional biodegradable structures fabricated by two-photon polymerization. Langmuir 25(5):3219–3223
Cooke MN et al (2003) Use of stereolithography to manufacture critical-sized 3D biodegradable scaffolds for bone ingrowth. J Biomed Mater Res B Appl Biomater 64(2):65–69
Cooper GM et al (2010) Inkjet-based biopatterning of bone morphogenetic protein-2 to spatially control calvarial bone formation. Tissue Eng A 16(5):1749–1759
Costantini M et al (2017) Microfluidic-enhanced 3D bioprinting of aligned myoblast-laden hydrogels leads to functionally organized myofibers in vitro and in vivo. Biomaterials 131:98–110
Cui X et al (2012a) Thermal inkjet printing in tissue engineering and regenerative medicine. Recent Pat Drug Deliv Formul 6(2):149–155
Cui X et al (2012b) Direct human cartilage repair using three-dimensional bioprinting technology. Tissue Eng A 18(11–12):1304–1312
Cui X et al (2012c) Synergistic action of fibroblast growth factor-2 and transforming growth factor-beta1 enhances bioprinted human neocartilage formation. Biotechnol Bioeng 109(9): 2357–2368
Cui X, Gao G, Yonezawa T, Dai G (2014) Human Cartilage Tissue Fabrication Using Three-dimensional Inkjet Printing Technology. J. Vis. Exp (88), e51294, https://doi.org/10.3791/51294
Cvetkovic C et al (2014) Three-dimensionally printed biological machines powered by skeletal muscle. Proc Natl Acad Sci 111(28):10125–10130
Dadbakhsh S et al (2014) Effect of SLM parameters on transformation temperatures of shape memory nickel titanium parts. Adv Eng Mater 16(9):1140–1146
Darsell J et al (2003) From CT scan to ceramic bone graft. J Am Ceram Soc 86(7):1076–1080
Dean D et al (2012) Continuous digital light processing (cDLP): highly accurate additive manufacturing of tissue engineered bone scaffolds: this paper highlights the main issues regarding the application of continuous digital light processing (cDLP) for the production of highly accurate PPF scaffolds with layers as thin as 60 μm for bone tissue engineering. Virt Phy Prototyp 7(1):13–24
Dellinger JG et al (2007) Robotic deposition of model hydroxyapatite scaffolds with multiple architectures and multiscale porosity for bone tissue engineering. J Biomed Mater Res A 82(2): 383–394
Di Bella C et al (2015) 3D bioprinting of cartilage for orthopedic surgeons: reading between the lines. Front Surg 2:39
Doyle K (2014) Bioprinting: from patches to parts. Genetic Engineering and Biotechnology Mary Ann Liebert, Inc. News 34(10) pp. 1, 34–35 https://doi.org/10.1089/gen.34.10.02
Duan B,Wang M (2010a) Customized Ca–P/PHBV nanocomposite scaffolds for bone tissue engineering: design, fabrication, surface modification and sustained release of growth factor Bin Duan, Min Wang J. R. Soc. Interface, https://doi.org/10.1098/rsif.2010.0127.focus. Published 26 May 2010
Duan B, Wang M (2010b) Encapsulation and release of biomolecules from ca–P/PHBV nano-composite microspheres and three-dimensional scaffolds fabricated by selective laser sintering. Polym Degrad Stab 95(9):1655–1664
Duan B et al (2010) Three-dimensional nanocomposite scaffolds fabricated via selective laser sintering for bone tissue engineering. Acta Biomater 6(12):4495–4505

Duan B, Hockaday L, Kang K, Butcher J (2013) 3D Bioprinting of heterogeneous aortic valve conduits with alginate/gelatin hydrogels. J Biomed Mater Res 101(5):1255–1264
Duan B, Kapetanovic E, Hockaday L, Butcher J (2014) 3D printed trileaflet valve conduits using biological hydrogels and human valve interstitial cells. Acta Biomater 10(5):1836–1846
Elomaa L et al (2011) Preparation of poly (ε-caprolactone)-based tissue engineering scaffolds by stereolithography. Acta Biomater 7(11):3850–3856
Elomaa L et al (2013) Porous 3D modeled scaffolds of bioactive glass and photocrosslinkable poly (ε-caprolactone) by stereolithography. Compos Sci Technol 74:99–106
Eosoly S et al (2010) Selective laser sintering of hydroxyapatite/poly-ε-caprolactone scaffolds. Acta Biomater 6(7):2511–2517
Eosoly S et al (2012) Interaction of cell culture with composition effects on the mechanical properties of polycaprolactone-hydroxyapatite scaffolds fabricated via selective laser sintering (SLS). Mater Sci Eng C 32(8):2250–2257
Eshraghi S, Das S (2010) Mechanical and microstructural properties of polycaprolactone scaffolds with one-dimensional, two-dimensional, and three-dimensional orthogonally oriented porous architectures produced by selective laser sintering. Acta Biomater 6(7):2467–2476
Fedorovich NE et al (2011) Biofabrication of osteochondral tissue equivalents by printing topologically defined, cell-laden hydrogel scaffolds. Tissue Eng Part C Methods 18(1):33–44
Fielding GA et al (2012) Effects of silica and zinc oxide doping on mechanical and biological properties of 3D printed tricalcium phosphate tissue engineering scaffolds. Dent Mater 28(2): 113–122
Forgacs G (2012) Perfusable vascular networks. Nat Mater 11:746–747
Freed LE et al (1993) Neocartilage formation in vitro and in vivo using cells cultured on synthetic biodegradable polymers. J Biomed Mater Res 27(1):11–23
Fu Q et al (2011) Direct ink writing of highly porous and strong glass scaffolds for load-bearing bone defects repair and regeneration. Acta Biomater 7(10):3547–3554
Gaebel R, Ma N, Liu J, Guan J, Koch L, Klopsch C, Gruene M, Toelk A, Wang W, Mark P, Wang F, Chichkov B, Li W, Steinhoff G (2011) Patterning human stem cells and endothelial cells with laser printing for cardiac regeneration. Biomaterials 32:9218–9230
Gao G et al (2014) Bioactive nanoparticles stimulate bone tissue formation in bioprinted three-dimensional scaffold and human mesenchymal stem cells. Biotechnol J 9(10):1304–1311
Gao G et al (2015a) Improved properties of bone and cartilage tissue from 3D inkjet-bioprinted human mesenchymal stem cells by simultaneous deposition and photocrosslinking in PEG-GelMA. Biotechnol Lett 37(11):2349–2355
Gao G et al (2015b) Inkjet-bioprinted acrylated peptides and PEG hydrogel with human mesenchymal stem cells promote robust bone and cartilage formation with minimal printhead clogging. Biotechnol J 10(10):1568–1577
Gao L, Kupfer M, Jung J, Yang L, Zhang P, Da Sie Y, Tran Q, Ajeti V, Freeman B, Fast V, Campagnola P, Ogle B, Zhang J (2017) Myocardial tissue engineering with cells derived from human-induced pluripotent stem cells and native-like high-resolution, 3-dimensionally printed scaffold. Circ Res 120:1318–1325
Gbureck U et al (2007a) Direct printing of bioceramic implants with spatially localized angiogenic factors. Adv Mater 19(6):795–800
Gbureck U et al (2007b) Low temperature direct 3D printed bioceramics and biocomposites as drug release matrices. J Control Release 122(2):173–180
Ge Z et al (2009) Proliferation and differentiation of human osteoblasts within 3D printed poly-lactic-co-glycolic acid scaffolds. J Biomater Appl 23(6):533–547
Geetha M et al (2009) Ti based biomaterials, the ultimate choice for orthopaedic implants–a review. Prog Mater Sci 54(3):397–425
Gibson I et al (2010) Additive manufacturing technologies. Springer, New York
Goodridge RD et al (2007) Biological evaluation of an apatite–mullite glass-ceramic produced via selective laser sintering. Acta Biomater 3(2):221–231

Gruene M et al (2010) Laser printing of stem cells for biofabrication of scaffold-free autologous grafts. Tissue Eng Part C Methods 17(1):79–87
Hedayati R et al (2017) How does tissue regeneration influence the mechanical behavior of additively manufactured porous biomaterials? J Mech Behav Biomed Mater 65:831–841
Heinl P et al (2008) Cellular Ti–6Al–4V structures with interconnected macro porosity for bone implants fabricated by selective electron beam melting. Acta Biomater 4(5):1536–1544
Heller C et al (2009) Vinyl esters: low cytotoxicity monomers for the fabrication of biocompatible 3D scaffolds by lithography based additive manufacturing. J Polym Sci A Polym Chem 47(24): 6941–6954
Heo SJ et al (2009) Fabrication and characterization of novel nano-and micro-HA/PCL composite scaffolds using a modified rapid prototyping process. J Biomed Mater Res A 89(1):108–116
Hockaday L, Kang K, Colangelo N, Cheung P, Duan B, Malone E, Wu J, Giradi L, Bonassar L, Lipson H, Chu C, Butcher J (2012) Rapid 3D printing of anatomically accurate and mechanically heterogeneous aortic valve hydrogel scaffolds. Biofabrication 4(3):035005
Hollister SJ (2005) Porous scaffold design for tissue engineering. Nat Mater 4(7):518–524
Hoque ME et al (2012) Extrusion based rapid prototyping technique: an advanced platform for tissue engineering scaffold fabrication. Biopolymers 97(2):83–93
Hsu S-h et al (2007) Evaluation of the growth of chondrocytes and osteoblasts seeded into precision scaffolds fabricated by fused deposition manufacturing. J Biomed Mater Res B Appl Biomater 80(2):519–527
Hsu S-h et al (2011) Chondrogenesis from human placenta-derived mesenchymal stem cells in three-dimensional scaffolds for cartilage tissue engineering. Tissue Eng A 17(11-12): 1549–1560
Hsu S-h et al (2012) Air plasma treated chitosan fibers-stacked scaffolds. Biofabrication 4(1): 015002
Hung KC et al (2014) Synthesis and 3D printing of biodegradable polyurethane elastomer by a water-based process for cartilage tissue engineering applications. Adv Healthc Mater 3(10): 1578–1587
Husmann I et al (1996) Growth factors in skeletal muscle regeneration. Cytokine Growth Factor Rev 7(3):249–258
Hutmacher DW (2000) Scaffolds in tissue engineering bone and cartilage. Biomaterials 21(24): 2529–2543
Hutmacher DW et al (2001) Mechanical properties and cell cultural response of polycaprolactone scaffolds designed and fabricated via fused deposition modeling. J Biomed Mater Res A 55(2): 203–216
Igawa K et al (2006) Tailor-made tricalcium phosphate bone implant directly fabricated by a three-dimensional ink-jet printer. J Artif Organs 9(4):234–240
Jansen J et al (2009) Fumaric acid monoethyl ester-functionalized poly (D, L-lactide)/N-vinyl-2-pyrrolidone resins for the preparation of tissue engineering scaffolds by stereolithography. Biomacromolecules 10(2):214–220
Jardini A et al (2011) Application of direct metal laser sintering in titanium alloy for cranioplasty. Brazilian conference on manufacturing engineering
Jose RR et al (2016) Evolution of bioinks and additive manufacturing technologies for 3D bioprinting. ACS Biomater Sci Eng 2(10):1662–1678
Kalita SJ et al (2003) Development of controlled porosity polymer-ceramic composite scaffolds via fused deposition modeling. Mater Sci Eng C 23(5):611–620
Kanczler JM et al (2009) Biocompatibility and osteogenic potential of human fetal femur-derived cells on surface selective laser sintered scaffolds. Acta Biomater 5(6):2063–2071
Kang H-W et al (2016) A 3D bioprinting system to produce human-scale tissue constructs with structural integrity. Nat Biotechnol 34(3):312–319
Kazimoğlu C et al (2003) A novel biodegradable PCL film for tendon reconstruction: Achilles tendon defect model in rats. Int J Artif Organs 26(9):804–812

Ker ED et al (2011) Bioprinting of growth factors onto aligned sub-micron fibrous scaffolds for simultaneous control of cell differentiation and alignment. Biomaterials 32(32):8097–8107
Keriquel V et al (2010) In vivo bioprinting for computer-and robotic-assisted medical intervention: preliminary study in mice. Biofabrication 2(1):014101
Kew S et al (2012) Synthetic collagen fascicles for the regeneration of tendon tissue. Acta Biomater 8(10):3723–3731
Khalil S et al (2005) Multi-nozzle deposition for construction of 3D biopolymer tissue scaffolds. Rapid Prototyp J 11(1):9–17
Khalyfa A et al (2007) Development of a new calcium phosphate powder-binder system for the 3D printing of patient specific implants. J Mater Sci Mater Med 18(5):909–916
Kim JY, Cho D-W (2009) The optimization of hybrid scaffold fabrication process in precision deposition system using design of experiments. Microsyst Technol 15(6):843–851
Kim Y, Kim G (2013) Collagen/alginate scaffolds comprising core (PCL)–shell (collagen/alginate) struts for hard tissue regeneration: fabrication, characterisation, and cellular activities. J Mater Chem B 1(25):3185–3194
Kim JY et al (2007) Development of a bone scaffold using HA nanopowder and micro-stereolithography technology. Microelectron Eng 84(5):1762–1765
Kim JH et al (2016) Three-dimensional cell-based bioprinting for soft tissue regeneration. Tissue Eng Regen Med 13(6):647–662
Klammert U et al (2010) 3D powder printed calcium phosphate implants for reconstruction of cranial and maxillofacial defects. J Cranio-Maxillofac Surg 38(8):565–570
Koch L et al (2012) Skin tissue generation by laser cell printing. Biotechnol Bioeng 109(7): 1855–1863
Kolan KC et al (2012) Effect of material, process parameters, and simulated body fluids on mechanical properties of 13-93 bioactive glass porous constructs made by selective laser sintering. J Mech Behav Biomed Mater 13:14–24
Kolesky D, Truby R, Gladman A, Busbee T, Homan K, Lewis J (2014) 3D Bioprinting of vascularized, heterogeneous cell-laden tissue constructs. Adv Mater 26:3124–3130
Kolesky D, Homan K, Skylar-Scott M, Lewis J (2016) Three-dimensional bioprinting of thick vascularized tissues. Proc Natl Acad Sci 113(12):3179–3184
Korpela J et al (2013) Biodegradable and bioactive porous scaffold structures prepared using fused deposition modeling. J Biomed Mater Res B Appl Biomater 101(4):610–619
Kruth J-P (1991) Material incress manufacturing by rapid prototyping techniques. CIRP Annals Manuf Technol 40(2):603–614
Kruth J-P et al (1998) Progress in additive manufacturing and rapid prototyping. CIRP Annals Manufa Technol 47(2):525–540
Kundu J et al (2015) An additive manufacturing-based PCL–alginate–chondrocyte bioprinted scaffold for cartilage tissue engineering. J Tissue Eng Regen Med 9(11):1286–1297
Lam CXF et al (2002) Scaffold development using 3D printing with a starch-based polymer. Mater Sci Eng C 20(1):49–56
Lam CX et al (2007) Comparison of the degradation of polycaprolactone and polycaprolactone–(β-tricalcium phosphate) scaffolds in alkaline medium. Polym Int 56(6):718–728
Lam CX et al (2008) Dynamics of in vitro polymer degradation of polycaprolactone-based scaffolds: accelerated versus simulated physiological conditions. Biomed Mater 3(3):034108
Lam C et al (2009a) Composite PLDLLA/TCP scaffolds for bone engineering: mechanical and in vitro evaluations. 13th International Conference on Biomedical Engineering, Springer
Lam CX et al (2009b) Evaluation of polycaprolactone scaffold degradation for 6 months in vitro and in vivo. J Biomed Mater Res A 90(3):906–919
Lan PX et al (2009) Development of 3D PPF/DEF scaffolds using micro-stereolithography and surface modification. J Mater Sci Mater Med 20(1):271–279
Lee JW et al (2007a) 3D scaffold fabrication with PPF/DEF using micro-stereolithography. Microelectron Eng 84(5):1702–1705

Lee K-W et al (2007b) Poly (propylene fumarate) bone tissue engineering scaffold fabrication using stereolithography: effects of resin formulations and laser parameters. Biomacromolecules 8(4): 1077–1084
Lee S-J et al (2008) Application of microstereolithography in the development of three-dimensional cartilage regeneration scaffolds. Biomed Microdevices 10(2):233–241
Lee JW et al (2009) Development of nano-and microscale composite 3D scaffolds using PPF/DEF-HA and micro-stereolithography. Microelectron Eng 86(4):1465–1467
Lee JW et al (2011) Bone regeneration using a microstereolithography-produced customized poly (propylene fumarate)/diethyl fumarate photopolymer 3D scaffold incorporating BMP-2 loaded PLGA microspheres. Biomaterials 32(3):744–752
Lee JS et al (2012) Effect of pore architecture and stacking direction on mechanical properties of solid freeform fabrication-based scaffold for bone tissue engineering. J Biomed Mater Res A 100(7):1846–1853
Lee H et al (2013) Cell-laden poly (ϵ-caprolactone)/alginate hybrid scaffolds fabricated by an aerosol cross-linking process for obtaining homogeneous cell distribution: fabrication, seeding efficiency, and cell proliferation and distribution. Tissue Eng Part C Methods 19(10):784–793
Leukers B et al (2005) Hydroxyapatite scaffolds for bone tissue engineering made by 3D printing. J Mater Sci Mater Med 16(12):1121–1124
Li X et al (2009) Fabrication and characterization of porous Ti6Al4V parts for biomedical applications using electron beam melting process. Mater Lett 63(3):403–405
Li J et al (2011) Fabrication of individual scaffolds based on a patient-specific alveolar bone defect model. J Biotechnol 151(1):87–93
Liang D et al (2007) Functional electrospun nanofibrous scaffolds for biomedical applications. Adv Drug Deliv Rev 59(14):1392–1412
Linzhong Z et al (2010) The research of technique on fabricating hydrogel scaffolds for cartilage tissue engineering based on stereo-lithography. Digital Manufacturing and Automation (ICDMA), 2010 International Conference on, IEEE
Liu L et al (2009) Multinozzle low-temperature deposition system for construction of gradient tissue engineering scaffolds. J Biomed Mater Res B Appl Biomater 88(1):254–263
Liu A et al (2016) 3D Printing Surgical Implants at the clinic: A Experimental Study on Anterior Cruciate Ligament Reconstruction. Sci Rep 6:21704; https://doi.org/10.1038/srep21704
Lode A et al (2014) Fabrication of porous scaffolds by three-dimensional plotting of a pasty calcium phosphate bone cement under mild conditions. J Tissue Eng Regen Med 8(9):682–693
Lohfeld S et al (2012) Fabrication, mechanical and in vivo performance of polycaprolactone/ tricalcium phosphate composite scaffolds. Acta Biomater 8(9):3446–3456
Lorrison J et al (2005) Processing of an apatite-mullite glass-ceramic and an hydroxyapatite/ phosphate glass composite by selective laser sintering. J Mater Sci Mater Med 16(8):775–781
Lu Y et al (2006) A digital micro-mirror device-based system for the microfabrication of complex, spatially patterned tissue engineering scaffolds. J Biomed Mater Res A 77(2):396–405
Luo Y et al (2015) Alginate/nanohydroxyapatite scaffolds with designed core/shell structures fabricated by 3D plotting and in situ mineralization for bone tissue engineering. ACS Appl Mater Interfaces 7(12):6541–6549
Lv J et al (2015a) Electron beam melting fabrication of porous Ti6Al4V scaffolds: cytocompatibility and osteogenesis. Adv Eng Mater 17(9):1391–1398
Lv J et al (2015b) Enhanced angiogenesis and osteogenesis in critical bone defects by the controlled release of BMP-2 and VEGF: implantation of electron beam melting-fabricated porous Ti6Al4V scaffolds incorporating growth factor-doped fibrin glue. Biomed Mater 10(3):035013
Ma L et al (2017) 3D printed personalized titanium plates improve clinical outcome in microwave ablation of bone tumors around the knee. Sci Rep 7, 7626; https://doi.org/10.1038/s41598-017-07243-3
Malda J et al (2013) 25th anniversary article: engineering hydrogels for biofabrication. Adv Mater 25(36):5011–5028

Marino A et al (2014) The Osteoprint: a bioinspired two-photon polymerized 3-D structure for the enhancement of bone-like cell differentiation. Acta Biomater 10(10):4304–4313
Martínez-Vázquez FJ et al (2010) Improving the compressive strength of bioceramic robocast scaffolds by polymer infiltration. Acta Biomater 6(11):4361–4368
Martins A et al (2009) Hierarchical starch-based fibrous scaffold for bone tissue engineering applications. J Tissue Eng Regen Med 3(1):37–42
McCarthy JC et al (1997) Custom and modular components in primary total hip replacement. Clin Orthop Relat Res 344:162–171
McCune M, Shafiee A, Forgacs G, Kosztin I (2014) Predictive modeling of post bioprinting structure formation. Soft Matter 10:1790–1800
Melchels FP et al (2009) A poly (D, L-lactide) resin for the preparation of tissue engineering scaffolds by stereolithography. Biomaterials 30(23):3801–3809
Melchels FP et al (2010) Effects of the architecture of tissue engineering scaffolds on cell seeding and culturing. Acta Biomater 6(11):4208–4217
Melchels FP et al (2012) Additive manufacturing of tissues and organs. Prog Polym Sci 37(8): 1079–1104
Merceron TK et al (2015) A 3D bioprinted complex structure for engineering the muscle–tendon unit. Biofabrication 7(3):035003
Mikos AG, Temenoff JS (2000) Formation of highly porous biodegradable scaffolds for tissue engineering. Electron J Biotechnol 3(2):23–24
Miller J, Stevens K, Yang M, Baker B, Nguyen D, Cohen D, Toro E, Chen A, Galie P, Yu X, Chaturvedi R, Bhatia S, Chen C (2012) Rapid casting of patterned vascular networks for perfusable engineered three-dimensional tissues. Nat Mater 11:768–774
Miranda P et al (2006) Sintering and robocasting of β-tricalcium phosphate scaffolds for orthopaedic applications. Acta Biomater 2(4):457–466
Miranda P et al (2008) Finite element modeling as a tool for predicting the fracture behavior of robocast scaffolds. Acta Biomater 4(6):1715–1724
Moldovan L, Babbey C, Murphy M, Moldovan N (2017) Comparison of Biomateria-dependent and -independent bioprinting methods for cardiovascular medicine. Curr Oponion Biomed Eng 2:124–131
Moroni L et al (2006) Polymer hollow fiber three-dimensional matrices with controllable cavity and shell thickness. Biomaterials 27(35):5918–5926
Mosadegh B, Xiong G, Dunham S, Min J (2015) Current progress in 3D printing for cardiovascular tissue engineering. Biomed Mater 10:034002
Mott EJ et al (2016) Digital micromirror device (DMD)-based 3D printing of poly (propylene fumarate) scaffolds. Mater Sci Eng C 61:301–311
Murphy SV, Atala A (2014) 3D bioprinting of tissues and organs. Nat Biotechnol 32(8):773–785
Murr L et al (2010) Next-generation biomedical implants using additive manufacturing of complex, cellular and functional mesh arrays. Philos Trans Royal Soc London A Math Phys Eng Sci 368 (1917):1999–2032
Murr L et al (2011) Microstructure and mechanical properties of open-cellular biomaterials prototypes for total knee replacement implants fabricated by electron beam melting. J Mech Behav Biomed Mater 4(7):1396–1411
Murr LE et al (2012) Next generation orthopaedic implants by additive manufacturing using electron beam melting. Int J Biomat 2012:14
Naing M et al (2005) Fabrication of customised scaffolds using computer-aided design and rapid prototyping techniques. Rapid Prototyp J 11(4):249–259
Nichol JW, Khademhosseini A (2009) Modular tissue engineering: engineering biological tissues from the bottom up. Soft Matter 5(7):1312–1319
Norotte C, Marga F, Niklason L, Forgacs G (2009) Scaffold-free vascular tissue engineering using bioprinting. Biomaterials 30(30):5910–5917
Oghbaei M, Mirzaee O (2010) Microwave versus conventional sintering: a review of fundamentals, advantages and applications. J Alloys Compd 494(1):175–189

Oh SH et al (2007) In vitro and in vivo characteristics of PCL scaffolds with pore size gradient fabricated by a centrifugation method. Biomaterials 28(9):1664–1671
Oliveira A et al (2009) Nucleation and growth of biomimetic apatite layers on 3D plotted biodegradable polymeric scaffolds: effect of static and dynamic coating conditions. Acta Biomater 5(5):1626–1638
Oliveira A et al (2012) Peripheral mineralization of a 3D biodegradable tubular construct as a way to enhance guidance stabilization in spinal cord injury regeneration. J Mater Sci Mater Med 23 (11):2821–2830
Oryan A et al (2013) A long-term in vivo investigation on the effects of xenogenous based, electrospun, collagen implants on the healing of experimentally-induced large tendon defects. J Musculoskelet Neuronal Interact 13(3):353–367
Ostrovidov S et al (2014) Skeletal muscle tissue engineering: methods to form skeletal myotubes and their applications. Tissue Eng Part B Rev 20(5):403–436
Ouyang HW et al (2003) Knitted poly-lactide-co-glycolide scaffold loaded with bone marrow stromal cells in repair and regeneration of rabbit Achilles tendon. Tissue Eng 9(3):431–439
Owen R et al (2016) Emulsion templated scaffolds with tunable mechanical properties for bone tissue engineering. J Mech Behav Biomed Mater 54:159–172
Ozbolat IT, Yu Y (2013) Bioprinting toward organ fabrication: challenges and future trends. IEEE Trans Biomed Eng 60(3):691–699
Padilla S et al (2007) Bioactive glass as precursor of designed-architecture scaffolds for tissue engineering. J Biomed Mater Res A 81(1):224–232
Palmquist A et al (2013) Long-term biocompatibility and osseointegration of electron beam melted, free-form–fabricated solid and porous titanium alloy: experimental studies in sheep. J Biomater Appl 27(8):1003–1016
Park JK et al (2011) Solid free-form fabrication of tissue-engineering scaffolds with a poly (lactic-co-glycolic acid) grafted hyaluronic acid conjugate encapsulating an intact bone morphogenetic protein–2/poly (ethylene glycol) complex. Adv Funct Mater 21(15):2906–2912
Parthasarathy J et al (2010) Mechanical evaluation of porous titanium (Ti6Al4V) structures with electron beam melting (EBM). J Mech Behav Biomed Mater 3(3):249–259
Pashneh-Tala S, McNeil S, Claeyssens F (2016) The tissue-engineered vascular graft- past, present, and future. Tissue Eng Part B 22(1):68–100
Pati F, Jang J, Ha D, Won K, Rhie J, Shim J, Kim D, Cho D (2013) Printing three-dimensional tissue analogues with decellularized extracellular matrix bioink. Nat Commun 5:3935
Patz T et al (2005) Two-dimensional differential adherence and alignment of C2C12 myoblasts. Mater Sci Eng B 123(3):242–247
Pereira TF et al (2012) 3D printing of poly (3-hydroxybutyrate) porous structures using selective laser sintering. Macromolecular Symposia, Wiley Online Library
Petrochenko PE et al (2015) Laser 3D printing with sub-microscale resolution of porous elastomeric scaffolds for supporting human bone stem cells. Adv Healthc Mater 4(5):739–747
Phillippi JA et al (2008) Microenvironments engineered by inkjet Bioprinting spatially direct adult stem cells toward muscle-and bone-like subpopulations. Stem Cells 26(1):127–134
Poldervaart MT et al (2013) Sustained release of BMP-2 in bioprinted alginate for osteogenicity in mice and rats. PLoS One 8(8):e72610
Poldervaart MT et al (2014) Prolonged presence of VEGF promotes vascularization in 3D bioprinted scaffolds with defined architecture. J Control Release 184:58–66
Ponader S et al (2010) In vivo performance of selective electron beam-melted Ti-6Al-4V structures. J Biomed Mater Res A 92(1):56–62
Qiao F et al (2015) Application of 3D printed customized external fixator in fracture reduction. Injury 46(6):1150–1155
Qiu Y et al (2013) In vitro two-dimensional and three-dimensional tenocyte culture for tendon tissue engineering. J Tissue Eng Regen Med 10(3):E216–E226
Rahimtoola ZO, Hubach P (2004) Total modular wrist prosthesis: a new design. Scand J Plast Reconstr Surg Hand Surg 38(3):160–165

Raman R et al (2016) High-resolution projection Microstereolithography for patterning of Neovasculature. Adv Healthc Mater 5(5):610–619
Ramanath H et al (2008) Melt flow behaviour of poly-ε-caprolactone in fused deposition modelling. J Mater Sci Mater Med 19(7):2541–2550
Ramón-Azcón J et al (2013) Dielectrophoretically aligned carbon nanotubes to control electrical and mechanical properties of hydrogels to fabricate contractile muscle myofibers. Adv Mater 25 (29):4028–4034
Rangarajan S et al (2014) Use of flow, electrical, and mechanical stimulation to promote engineering of striated muscles. Ann Biomed Eng 42(7):1391–1405
Razal JM et al (2009) Wet-spun biodegradable fibers on conducting platforms: novel architectures for muscle regeneration. Adv Funct Mater 19(21):3381–3388
Regeneration T (2015) Understanding tissue physiology and development to engineer functional substitutes. Academic Press, Cambridge, MA
Rengier F et al (2010) 3D printing based on imaging data: review of medical applications. Int J Comput Assist Radiol Surg 5(4):335–341
Resnina N et al (2013) Influence of chemical composition and pre-heating temperature on the structure and martensitic transformation in porous TiNi-based shape memory alloys, produced by self-propagating high-temperature synthesis. Intermetallics 32:81–89
Ronca A et al (2013) Preparation of designed poly (D, L-lactide)/nanosized hydroxyapatite composite structures by stereolithography. Acta Biomater 9(4):5989–5996
Russias J et al (2007) Fabrication and in vitro characterization of three-dimensional organic/inorganic scaffolds by robocasting. J Biomed Mater Res A 83(2):434–445
Sahoo S et al (2006) Characterization of a novel polymeric scaffold for potential application in tendon/ligament tissue engineering. Tissue Eng 12(1):91–99
Sahoo S et al (2010) A bFGF-releasing silk/PLGA-based biohybrid scaffold for ligament/tendon tissue engineering using mesenchymal progenitor cells. Biomaterials 31(11):2990–2998
Saijo H et al (2009) Maxillofacial reconstruction using custom-made artificial bones fabricated by inkjet printing technology. J Artif Organs 12(3):200–205
Samad WZ, Salleh MM, Shafiee A, Yarmo MA (2010a) Transparent conducting thin films of fluoro doped tin oxide (FTO) deposited using inkjet printing technique. IEEE Int Conf Semicond Elec 52–55
Samad WZ, Salleh MM, Shafiee A, Yarmo MA (2010b) Preparation nanostructure thin films of fluorine doped tin oxide by inkjet printing technique. AIP Conf Proc 1284:83–86
Samad WZ, Salleh MM, Shafiee A, Yarmo MA (2010c) Transparent conductive electrode of fluorine doped tin oxide prepared by inkjet printing technique. Material Science Forum 663 (665:694–697
Samad WZ, Salleh MM, Shafiee A, Yarmo MA (2011) Structural, optical and electrical properties of fluorine doped tin oxide thin films deposited using inkjet printing technique. Sains Malaysiana 40(3):251–257
San Choi J et al (2008) The influence of electrospun aligned poly (ϵ-caprolactone)/collagen nanofiber meshes on the formation of self-aligned skeletal muscle myotubes. Biomaterials 29 (19):2899–2906
Santos CF et al (2012) Design and production of sintered β-tricalcium phosphate 3D scaffolds for bone tissue regeneration. Mater Sci Eng C 32(5):1293–1298
Santos ARC et al (2013) Additive manufacturing techniques for scaffold-based cartilage tissue engineering: a review on various additive manufacturing technologies in generating scaffolds for cartilage tissue engineering. Virtual Phy Prototyp 8(3):175–186
Sato M et al (2000) Reconstruction of rabbit Achilles tendon with three bioabsorbable materials: histological and biomechanical studies. J Orthop Sci 5(3):256–267
Schantz J-T et al (2003) Repair of calvarial defects with customised tissue-engineered bone grafts II. Evaluation of cellular efficiency and efficacy in vivo. Tissue Eng 9(4, Supplement 1):127–139
Schüller-Ravoo S et al (2013) Flexible and elastic scaffolds for cartilage tissue engineering prepared by Stereolithography using poly (trimethylene carbonate)-based resins. Macromol Biosci 13 (12):1711–1719

Schuurman W et al (2013) Gelatin-methacrylamide hydrogels as potential biomaterials for fabrication of tissue-engineered cartilage constructs. Macromol Biosci 13(5):551–561
Seck TM et al (2010) Designed biodegradable hydrogel structures prepared by stereolithography using poly (ethylene glycol)/poly (D, L-lactide)-based resins. J Control Release 148(1):34–41
Seitz H et al (2005) Three-dimensional printing of porous ceramic scaffolds for bone tissue engineering. J Biomed Mater Res B Appl Biomater 74(2):782–788
Seol YJ et al (2013) A new method of fabricating robust freeform 3D ceramic scaffolds for bone tissue regeneration. Biotechnol Bioeng 110(5):1444–1455
Seol Y-J et al (2014) Bioprinting technology and its applications. In: European journal of cardiothoracic surgery 46(3):342–348, https://doi.org/10.1093/ejcts/ezu148
Serra T et al (2013) High-resolution PLA-based composite scaffolds via 3-D printing technology. Acta Biomater 9(3):5521–5530
Seyednejad H et al (2012) In vivo biocompatibility and biodegradation of 3D-printed porous scaffolds based on a hydroxyl-functionalized poly (ε-caprolactone). Biomaterials 33(17): 4309–4318
Shafiee A, Atala A (2016) Printing technologies for medical applications. Trends Mol Med 22:245–265
Shafiee A, Atala A (2017) Tissue engineering: toward a new era of medicine. Annu Rev Med 68:29–40
Shafiee A, Salleh MM, Yahaya M (2008) Fabrication of organic solar cells based on a blend of donor-acceptor molecules by inkjet printing technique. IEEE Int Conf Semicond Elect 2008:319–322
Shafiee A, Mat Salleh M, Yahaya M (2009) Fabrication of organic solar cells based on a blend of poly (3-octylthiophene-2, 5-diyl) and fullerene derivative using inkjet printing technique. Proc SPIE 7493:74932D
Shafiee A, McCune M, Forgacs G, Kosztin I (2015) Post-deposition bioink self-assembly: a quantitative study. Biofabrication 7:045005
Shafiee A, Norotte C, Ghadiri E (2017) Cellular bioink surface tension: a tunable biophysical parameter for faster bioprinted-tissue maturation. Bioprinting 8(C):13–21
Sharma B, Elisseeff JH (2004) Engineering structurally organized cartilage and bone tissues. Ann Biomed Eng 32(1):148–159
Shen W et al (2012) Allogenous tendon stem/progenitor cells in silk scaffold for functional shoulder repair. Cell Transplant 21(5):943–958
Sherwood JK et al (2002) A three-dimensional osteochondral composite scaffold for articular cartilage repair. Biomaterials 23(24):4739–4751
Shim J-H et al (2012) Bioprinting of a mechanically enhanced three-dimensional dual cell-laden construct for osteochondral tissue engineering using a multi-head tissue/organ building system. J Micromech Microeng 22(8):085014
Shishkovsky I et al (2010) Porous titanium and nitinol implants synthesized by SHS/SLS: microstructural and histomorphological analyses of tissue reactions. Int J Self Propag High Temp Synth 19(2):157–167
Shor L et al (2005) Precision extruding deposition of composite polycaprolactone/hydroxyapatite scaffolds for bone tissue engineering. Bioengineering conference, 2005. Proceedings of the IEEE 31st annual northeast. In: IEEE
Shor L et al (2007) Fabrication of three-dimensional polycaprolactone/hydroxyapatite tissue scaffolds and osteoblast-scaffold interactions in vitro. Biomaterials 28(35):5291–5297
Shor L et al (2009) Precision extruding deposition (PED) fabrication of polycaprolactone (PCL) scaffolds for bone tissue engineering. Biofabrication 1(1):015003
Shuai C et al (2013) In vitro bioactivity and degradability of β-tricalcium phosphate porous scaffold fabricated via selective laser sintering. Biotechnol Appl Biochem 60(2):266–273
Simpson RL et al (2008) Development of a 95/5 poly (L-lactide-co-glycolide)/hydroxylapatite and β-tricalcium phosphate scaffold as bone replacement material via selective laser sintering. J Biomed Mater Res B Appl Biomater 84(1):17–25
Sobral JM et al (2011) Three-dimensional plotted scaffolds with controlled pore size gradients: effect of scaffold geometry on mechanical performance and cell seeding efficiency. Acta Biomater 7(3):1009–1018

Standard A (2012) F2792. 2012. Standard terminology for additive manufacturing technologies. ASTM International. See www.astm.org, West Conshohocken. https://doi.org/10.1520/F2792-12
Stübinger S et al (2013) Histological and biomechanical analysis of porous additive manufactured implants made by direct metal laser sintering: a pilot study in sheep. J Biomed Mater Res B Appl Biomater 101(7):1154–1163
Sudarmadji N et al (2011) Investigation of the mechanical properties and porosity relationships in selective laser-sintered polyhedral for functionally graded scaffolds. Acta Biomater 7(2): 530–537
Sun AX et al (2015) Projection stereolithographic fabrication of human adipose stem cell-incorporated biodegradable scaffolds for cartilage tissue engineering. Front Bioeng Biotechnol 3:115
Suwanprateeb J, Chumnanklang R (2006) Three-dimensional printing of porous polyethylene structure using water-based binders. J Biomed Mater Res B Appl Biomater 78(1):138–145
Suwanprateeb J et al (2008) Fabrication of bioactive hydroxyapatite/bis-GMA based composite via three dimensional printing. J Mater Sci Mater Med 19(7):2637–2645
Suwanprateeb J et al (2009) Mechanical and in vitro performance of apatite–wollastonite glass ceramic reinforced hydroxyapatite composite fabricated by 3D-printing. J Mater Sci Mater Med 20(6):1281
Suwanprateeb J et al (2012) Development of porous powder printed high density polyethylene for personalized bone implants. J Porous Mater 19(5):623–632
Tan H et al (2009) Injectable in situ forming biodegradable chitosan–hyaluronic acid based hydrogels for cartilage tissue engineering. Biomaterials 30(13):2499–2506
Tarafder S et al (2013a) Microwave-sintered 3D printed tricalcium phosphate scaffolds for bone tissue engineering. J Tissue Eng Regen Med 7(8):631–641
Tarafder S et al (2013b) 3D printed tricalcium phosphate bone tissue engineering scaffolds: effect of SrO and MgO doping on in vivo osteogenesis in a rat distal femoral defect model. Biomater Sci 1(12):1250–1259
Tartarisco G et al (2009) Polyurethane unimorph bender microfabricated with pressure assisted Microsyringe (PAM) for biomedical applications. Mater Sci Eng C 29(6):1835–1841
Tellis B et al (2008) Trabecular scaffolds created using micro CT guided fused deposition modeling. Mater Sci Eng C 28(1):171–178
Temenoff JS, Mikos AG (2000) Review: tissue engineering for regeneration of articular cartilage. Biomaterials 21(5):431–440
Tesavibul P et al (2012) Processing of 45S5 Bioglass® by lithography-based additive manufacturing. Mater Lett 74:81–84
Thavornyutikarn B et al (2014) Bone tissue engineering scaffolding: computer-aided scaffolding techniques. Progress Biomat 3(2-4):61–102
Thomsen P et al (2009) Electron beam-melted, free-form-fabricated titanium alloy implants: material surface characterization and early bone response in rabbits. J Biomed Mater Res B Appl Biomater 90(1):35–44
Tosun G, Tosun N (2012) Analysis of process parameters for porosity in porous NiTi implants. Mater Manuf Process 27(11):1184–1188
Tosun G et al (2009) A study on microstructure and porosity of NiTi alloy implants produced by SHS. J Alloys Compd 487(1):605–611
Tosun G et al (2012) Investigation of combustion channel in fabrication of porous NiTi alloy implants by SHS. Mater Lett 66(1):138–140
Traini T et al (2008) Direct laser metal sintering as a new approach to fabrication of an isoelastic functionally graded material for manufacture of porous titanium dental implants. Dent Mater 24(11):1525–1533
Travitzky N et al (2014) Additive manufacturing of ceramic-based materials. Adv Eng Mater 16(6): 729–754
Vaezi M et al (2013) A review on 3D micro-additive manufacturing technologies. Int J Adv Manuf Technol 67(5-8):1721–1754

Van Bael S et al (2013) In vitro cell-biological performance and structural characterization of selective laser sintered and plasma surface functionalized polycaprolactone scaffolds for bone regeneration. Mater Sci Eng C 33(6):3404–3412
van Hengel IA et al (2017) Selective laser melting porous metallic implants with immobilized silver nanoparticles kill and prevent biofilm formation by methicillin-resistant Staphylococcus aureus. Biomaterials 140:1–15
Ventola CL (2014) Medical applications for 3D printing: current and projected uses. PT 39(10): 704–711
Verdiyeva G et al (2015) Tendon reconstruction with tissue engineering approach – a review. J Biomed Nanotechnol 11(9):1495–1523
Vorndran E et al (2008) 3D powder printing of β-tricalcium phosphate ceramics using different strategies. Adv Eng Mater 10(12):B67–B71
Vozzi G et al (2002) Microsyringe-based deposition of two-dimensional and three-dimensional polymer scaffolds with a well-defined geometry for application to tissue engineering. Tissue Eng 8(6):1089–1098
Vozzi G et al (2003) Fabrication of PLGA scaffolds using soft lithography and microsyringe deposition. Biomaterials 24(14):2533–2540
Wang F et al (2004) Precision extruding deposition and characterization of cellular poly-ϵ-caprolactone tissue scaffolds. Rapid Prototyp J 10(1):42–49
Wang PY et al (2012) The roles of RGD and grooved topography in the adhesion, morphology, and differentiation of C2C12 skeletal myoblasts. Biotechnol Bioeng 109(8):2104–2115
Wang L et al (2015) Nanofiber yarn/hydrogel core–shell scaffolds mimicking native skeletal muscle tissue for guiding 3D myoblast alignment, elongation, and differentiation. ACS Nano 9(9): 9167–9179
Wang X et al (2017) 3D printing of polymer matrix composites: a review and prospective. Compos Part B 110:442–458
Webb WR et al (2013) The application of poly (3-hydroxybutyrate-co-3-hydroxyhexanoate) scaffolds for tendon repair in the rat model. Biomaterials 34(28):6683–6694
Weinberger F, Mannhardt I, Eschenhagen T (2017) Engineering cardiac muscle tissue- a maturating field of research. Circ Res 120:1487–1500
Weiß T et al (2009) Two-photon polymerization for microfabrication of three-dimensional scaffolds for tissue engineering application. Eng Life Sci 9(5):384–390
Weiß T et al (2011) Two-photon polymerization of biocompatible photopolymers for Micro-structured 3D Biointerfaces. Adv Eng Mater 13(9):B264–B273
Williams JM et al (2005) Bone tissue engineering using polycaprolactone scaffolds fabricated via selective laser sintering. Biomaterials 26(23):4817–4827
Winkel A et al (2012) Sintering of 3D-printed glass/HAp composites. J Am Ceram Soc 95(11): 3387–3393
Wiria F et al (2007) Poly-ε-caprolactone/hydroxyapatite for tissue engineering scaffold fabrication via selective laser sintering. Acta Biomater 3(1):1–12
Wiria FE et al (2010) Printing of titanium implant prototype. Mater Des 31:S101–S105
Wohlers T, Gornet T (2014) History of additive manufacturing. Wohlers Report 24:2014
Wong KV, Hernandez A (2012) International Scholarly Research Network. ISRN Mechanical Engineering 2012:10, https://doi.org/10.5402/2012/208760
Woodfield TB et al (2004) Design of porous scaffolds for cartilage tissue engineering using a three-dimensional fiber-deposition technique. Biomaterials 25(18):4149–4161
Wu W, DeConinck A, Lewis J (2011) Omnidirectional printing of 3D microvascular networks. Adv Health Mat 23:178–183
Wu SH et al (2013) Porous Titanium-6 Aluminum-4 vanadium cage has better Osseointegration and less Micromotion than a poly-ether-ether-ketone cage in sheep vertebral fusion. Artif Organs 37(12):E191–E201
Wu Y et al (2015) Direct E-jet printing of three-dimensional fibrous scaffold for tendon tissue engineering. J Biomed Mater Res B Appl Biomater 105:(3):616–627

Xiong Z et al (2001) Fabrication of porous poly (L-lactic acid) scaffolds for bone tissue engineering via precise extrusion. Scr Mater 45(7):773–779
Xiong Z et al (2002) Fabrication of porous scaffolds for bone tissue engineering via low-temperature deposition. Scr Mater 46(11):771–776
Xu T et al (2012) Hybrid printing of mechanically and biologically improved constructs for cartilage tissue engineering applications. Biofabrication 5(1):015001
Xu T et al (2013a) Complex heterogeneous tissue constructs containing multiple cell types prepared by inkjet printing technology. Biomaterials 34(1):130–139
Xu Y et al (2013b) Fabrication of electrospun poly (L-Lactide-co-ϵ-Caprolactone)/collagen Nanoyarn network as a novel, three-dimensional, Macroporous, aligned scaffold for tendon tissue engineering. Tissue Eng Part C Methods 19(12):925–936
Yang SS et al (2015) Fabrication of an osteochondral graft with using a solid freeform fabrication system. Tissue Eng Regener Med 12(4):239–248
Ye L et al (2010) Fabrication and biocompatibility of nano non-stoichiometric apatite and poly (ε-caprolactone) composite scaffold by using prototyping controlled process. J Mater Sci Mater Med 21(2):753–760
Yen H-J et al (2008) Fabrication of precision scaffolds using liquid-frozen deposition manufacturing for cartilage tissue engineering. Tissue Eng A 15(5):965–975
Yen H-J et al (2009) Evaluation of chondrocyte growth in the highly porous scaffolds made by fused deposition manufacturing (FDM) filled with type II collagen. Biomed Microdevices 11(3):615–624
Yeo M et al (2016) Combining a micro/nano-hierarchical scaffold with cell-printing of myoblasts induces cell alignment and differentiation favorable to skeletal muscle tissue regeneration. Biofabrication 8(3):035021
Yildirim ED et al (2010) Accelerated differentiation of osteoblast cells on polycaprolactone scaffolds driven by a combined effect of protein coating and plasma modification. Biofabrication 2(1):014109
Zadpoor AA, Malda J (2017) Ann Biomed Eng 45:1, https://doi.org/10.1007/s10439-016-1719-y
Zhang H et al (2008) Microassembly fabrication of tissue engineering scaffolds with customized design. IEEE Trans Autom Sci Eng 5(3):446–456
Zhang Y et al (2009) In vitro biocompatibility of hydroxyapatite-reinforced polymeric composites manufactured by selective laser sintering. J Biomed Mater Res A 91(4):1018–1027
Zhang Q et al (2013) In situ controlled release of rhBMP-2 in gelatin-coated 3D porous poly (ε-caprolactone) scaffolds for homogeneous bone tissue formation. Biomacromolecules 15(1):84–94
Zhao S et al (2016) The influence of cell morphology on the compressive fatigue behavior of Ti-6Al-4V meshes fabricated by electron beam melting. J Mech Behav Biomed Mater 59:251–264
Zhou Y et al (2007) In vitro bone engineering based on polycaprolactone and polycaprolactone–tricalcium phosphate composites. Polym Int 56(3):333–342
Zhou X et al (2016) Improved human bone marrow mesenchymal stem cell osteogenesis in 3D Bioprinted tissue scaffolds with low intensity pulsed ultrasound stimulation. Sci Rep 6:12